DESIGN AND EVALUATION OF AN AUDIO-FREQUENCY TRANSRESISTANCE AMPLIFIER FOR MAGNETIC TAPE PLAYBACK

A thesis submitted in partial fulfillment

of the requirements for the degree of

Master of Science in Engineering

By

THOMAS R. SALVATIERRA

B.E.E., University of Dayton, 2001

2011

Wright State University

WRIGHT STATE UNIVERSITY

SCHOOL OF GRADUATE STUDIES

August 3, 2010

I HEREBY RECOMMEND THAT THE THESIS PREPARED UNDER MY SUPERVISION BY Thomas R. Salvatierra ENTITLED Design and Evaluation of an Audio-Frequency Transresistance Amplifier for Magnetic Tape Playback BE ACCEPTED IN PARTIAL FULFILLMENT OF THE REQUIREMENTS FOR THE DEGREE OF Master of Science in Engineering.

Marian K. Kazimierczuk, Ph.D.
Thesis Director

Kefu Xue, Ph.D.
Department Chair

Committee on
Final Examination

Fred D. Garber, Ph.D.

Marian K. Kazimierczuk, Ph.D.

Raymond E. Siferd, Ph.D.

Andrew T. Hsu, Ph.D.
Dean, School of Graduate Studies

Abstract

Salvatierra, Thomas R. M.S.Egr., Department of Electrical Engineering, Wright State University, 2011. *Design and Evaluation of an Audio-Frequency Transresistance Amplifier for Magnetic Tape Playback.*

Analog magnetic tape remains a medium of choice for high-fidelity sound recording and reproduction. Some of this fidelity is sacrificed during the tape playback process; an optimized playback preamplifier is therefore critical to the performance of the medium. Existing playback methods integrate the voltage generated across the reproduce head to obtain a signal directly proportional to the remanent magnetic flux of the tape. An alternate playback method proposes the use of a transresistance amplifier to convert flux-proportional reproduce head current directly to voltage. This eliminates the need for voltage integration and minimizes the amount of equalization performed upon playback. Circuit size and complexity are likewise reduced. A practical transresistance playback preamplifier is designed and its performance is evaluated against selected integrating playback preamplifiers. SPICE simulation verifies that the proposed design offers a significant reduction in harmonic distortion, as well as improved transient response, magnitude response, and phase margin.

Contents

List of Figures

List of Tables

Acknowledgements

The author wishes to thank the following individuals:

Dr. Marian Kazimierczuk, for his critical guidance, encouragement, and patience;

Dr. Joe Tritschler, whose advice, insight, and willingness to share the results of prior research made this thesis possible;

Wes Earick, Mr. Phil Flynn of Wright State University Libraries, Mr. John French of JRF Magnetic Sciences, Inc., Dr. Nisha Kondrath, Julie Lee, Dr. Dakshina Murthy Bellur, and Tony Tritschler for providing invaluable technical assistance.

1 Introduction

1.1 Relevance of Analog Sound Recording in the Digital Age

The past two decades have seen digital technology gradually replace its analog counterparts in most areas of the professional audio market. However, many sound engineers, recording studios, and high-fidelity audio enthusiasts remain proponents of analog magnetic tape as a recording and playback medium [1], [2]. When judged solely upon the subjective *musical* qualities of audio signal reproduction, analog tape often yields results preferable to digital mediums [1], [3]. Accordingly, there exists an ongoing demand for improvements in analog sound reproduction technology among a portion of the market willing to pay for it.

1.2 Thesis Objectives

This thesis investigates potential improvements to the way in which audio data stored on analog magnetic tape is electronically retrieved or "played-back". It has been hypothesized that playback fidelity may be increased through the use of a transresistance amplifier instead of an integrating voltage amplifier. The concept explored herein was first introduced by Boegli in 1960 [4] and later mentioned by Perandi in 1991 [5]. Specific groundwork for this application was provided by Tritschler in a 2000 paper entitled *An Improved Playback Amplifier for High-Fidelity Analog Recording Systems* [6]. However, none of the previous work contains a detailed analysis of implementation and performance. Boegli and Tritschler likewise suggest further improvements that may be made to the basic design.

The goal of this research is to compile previously-unpublished information useful in the design of analog magnetic tape playback devices. Specific thesis objectives are:

1. To develop a generalized topology for a practical transresistance playback preamplifier.
2. To propose a design procedure for the transresistance playback preamplifier.
3. To simulate the circuit in SPICE and quantify performance.
4. To compare simulated performance to that of comparable existing designs.
5. To identify specific advantages and disadvantages of the proposed design.
6. To propose further work that may be undertaken regarding this subject.

2 Limitations of Existing Playback Topologies

2.1 Principles of Analog Magnetic Tape Playback

Audio signals recorded to magnetic tape are stored via a thin layer of ferromagnetic oxide applied to one side of a plastic film substrate. The ferromagnetic oxide consists of magnetic particles, or *domains,* which behave like miniature permanent magnets, as illustrated in Fig. 1 [3].

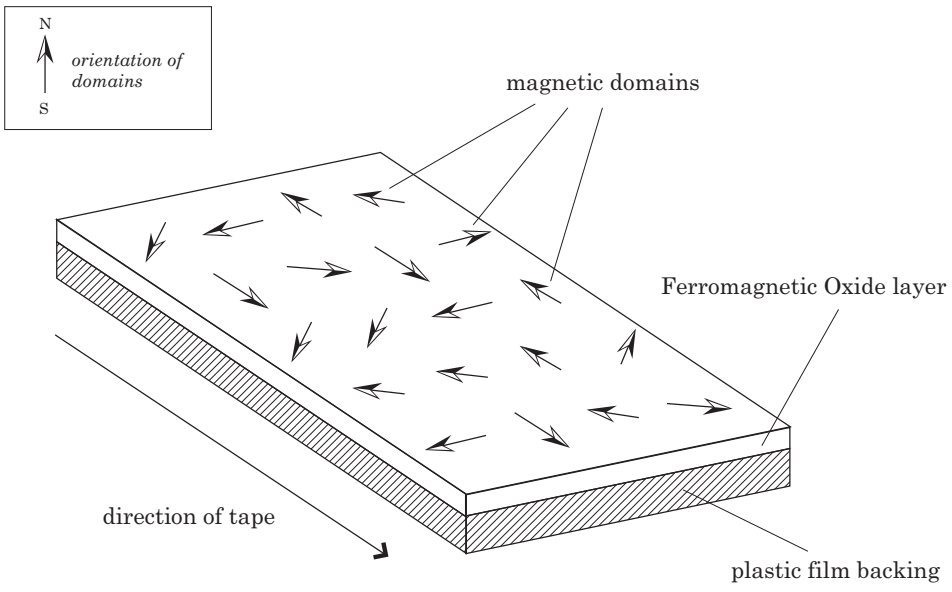

Figure 1: Magnetic tape surface.

The recording process sets the angular orientation of these domains on the tape's surface, establishing a relative magnetic field strength or *remanent magnetic flux* in direct proportion to the original signal as depicted in Fig. 2.

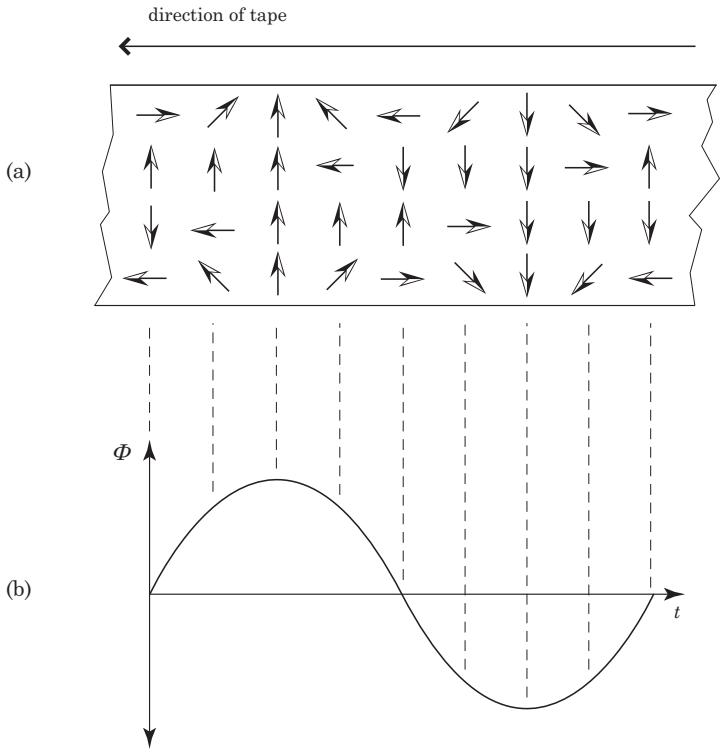

Figure 2: Magnetic flux encoding. (a) Orientation of magnetic domains on tape surface. (b) Equivalent time-varying magnetic flux signal $\phi(t)$.

Upon playback, the lateral motion of the tape at constant velocity generates an alternating magnetic flux $\phi(t)$, which is then introduced across the gap of an inductive transducer or *reproduce head*. The flux produces a proportional current in the windings of the head and a voltage between its two terminals. This voltage signal is then amplified, filtered, and fed to a line-level amplifier, eventually driving a power amplifier and loudspeaker. The standard playback preamplification scheme consists of four basic elements:

- Reproduce head
- Voltage amplifier
- Voltage integrator
- Equalization network

A block diagram of this approach is shown in Fig. 3.

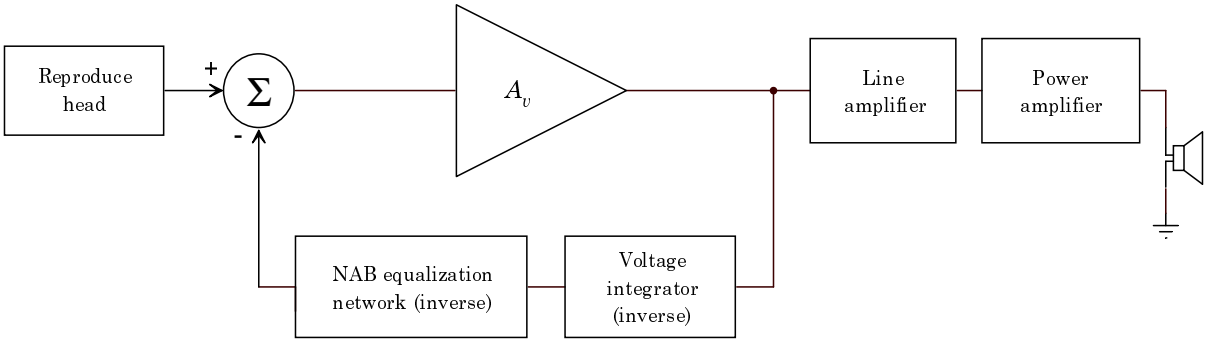

Figure 3: Block diagram of standard playback approach.

2.1.1 Reproduce Head

The reproduce head is an electromagnetic transducer consisting of a gapped magnetic core and a winding, depicted in Fig. 4 [3]. As the tape passes over the gap, the change in magnetic flux is mirrored within the core, inducing a current in the windings and a voltage across the terminals of the head. Since the reproduce head itself is essentially an inductor, Faraday's Law defines this voltage as

$$v_s(t) = N\frac{d\phi}{dt} \tag{2.1}$$

where N is the number of turns in the winding and $\frac{d\phi}{dt}$ is the rate of change of flux with respect to time as seen by the gap. As audio applications generally utilize voltage rather than current as the signal of interest, standard playback topologies sample $v_s(t)$ directly as the desired output of the reproduce head. This voltage, however, contains the differential component $\frac{d\phi}{dt}$ which results in a first-order rise (+6 dB per octave or +20 dB per decade) across the audio frequency spectrum as shown in Fig. 5. The resulting high-frequency boost must be compensated for by means of additional circuitry, as described in Section 2.1.3.

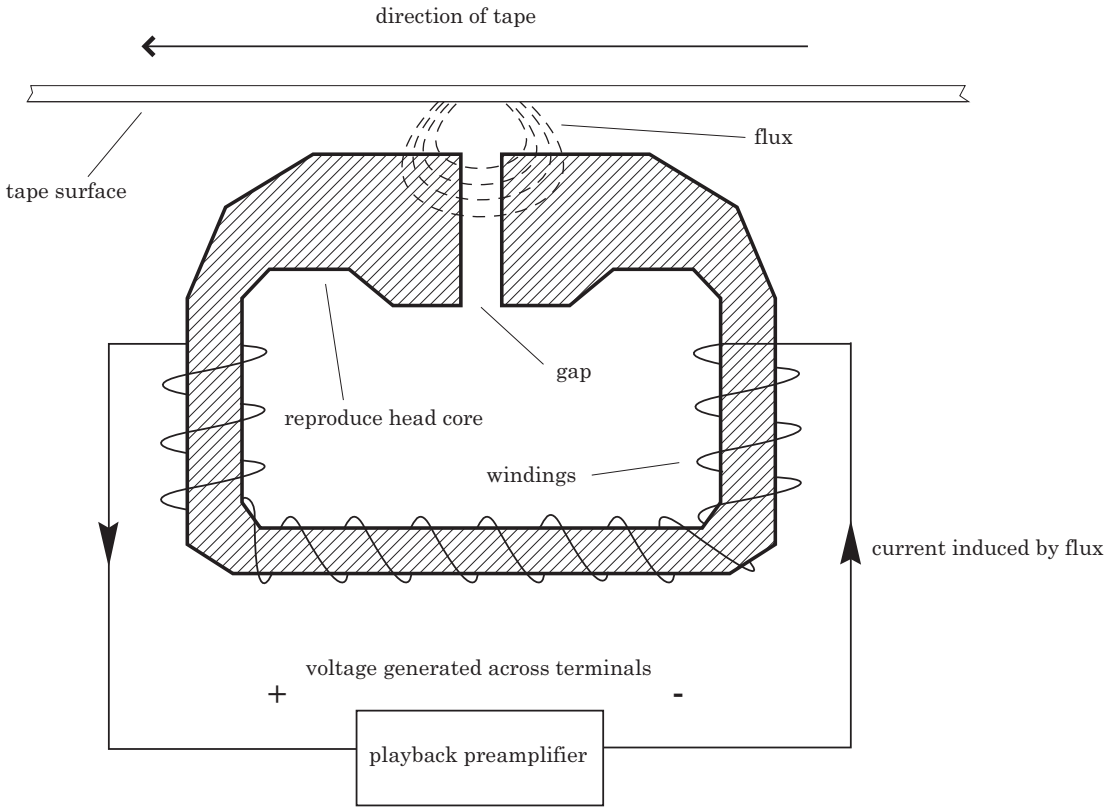

Figure 4: Reproduce head.

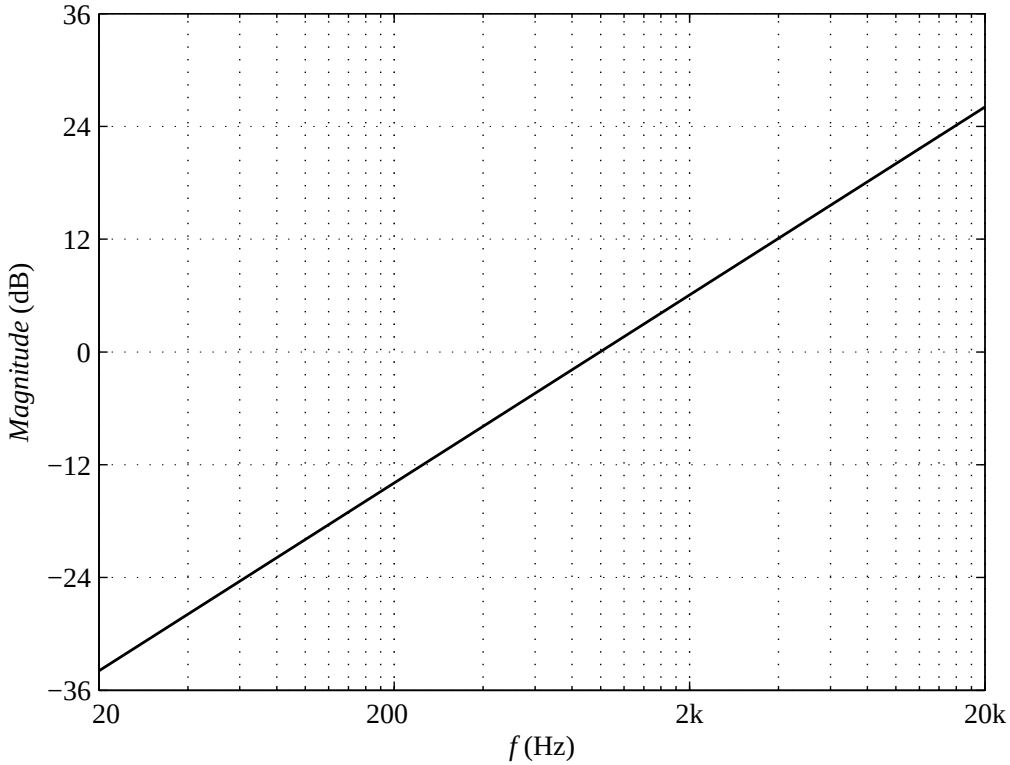

Figure 5: Differential component of reproduce head voltage.

2.1.2 Voltage Amplifier

The nominal output voltage of professional-grade reproduce heads is typically less than 4 mV(rms) [7], [8]. A high-gain, low-noise stage is therefore necessary to provide at least 20 dB of voltage gain before the signal may be run to a separate line-level amplifier stage [8]. This 20-dB boost is typically accomplished via a discrete three-stage cascaded negative feedback amplifier [9] or a non-inverting op-amp [10]. Selected designs also utilize a step-up transformer at the input to alleviate a portion of the initial high-gain requirement [11]. Fig. 6 illustrates some common topologies. As with any high-fidelity preamplifier, the gain stage itself must provide a flat response across the audio spectrum, typically 20 Hz to 20 kHz or the nominal range of human hearing [8]. This must be done while introducing as little noise and non-linear distortion as possible.

2.1.3 Voltage Integrator

As discussed in Section 2.1.1, the signal of interest $v_s(t)$ contains a differential component. In order to compensate for the first-order boost introduced by the differential of Fig. 5, a voltage integrator is utilized to attenuate the signal at the same rate. The integration characteristic is shown in Fig. 7. Voltage integration is provided by means of a capacitor within the feedback loop of the voltage amplifier as shown in Fig. ; the resulting post-integration transfer characteristic is therefore nominally flat.

2.1.4 Equalization Network

All analog tape recording and playback equipment marketed for commercial use in the United States must conform to equalization standards set by the National Association of Broadcasters (NAB). This is done as a means of compensating for imperfections in the frequency response of the tape medium itself, particularly in the high end [12], [8], [13]. Recording and playback must therefore be performed with respective NAB

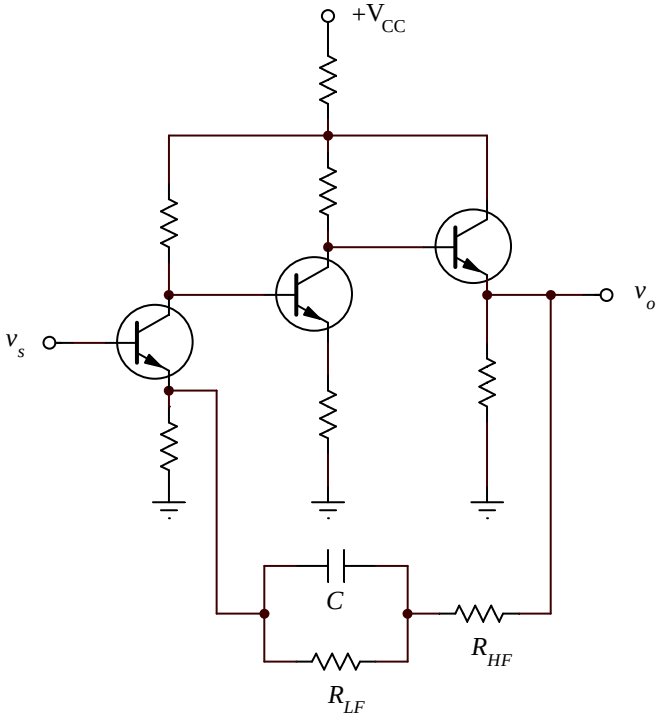

(a)

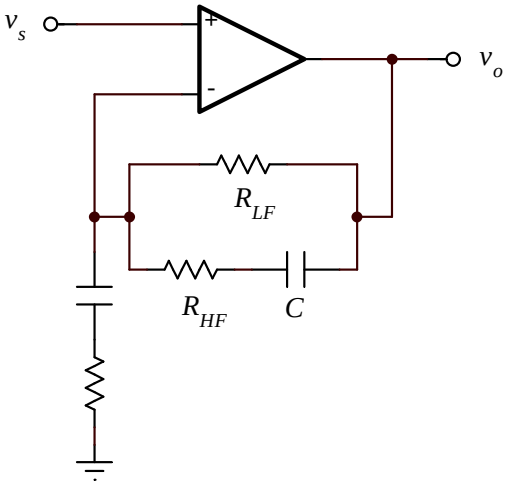

(b)

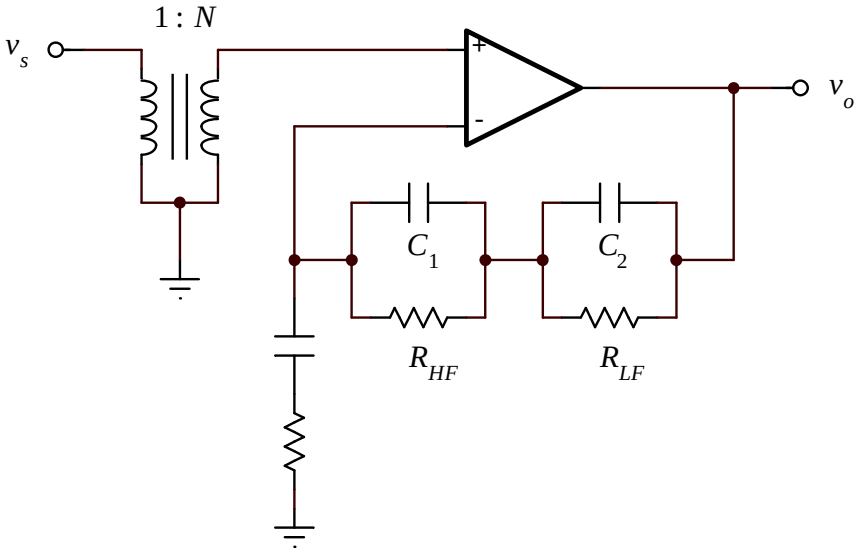

(c)

Figure 6: Common playback preamplifier approaches. (a) Discrete cascaded negative feedback amplifier. (b) Non-inverting op-amp. (c) Op-amp with step-up transformer.

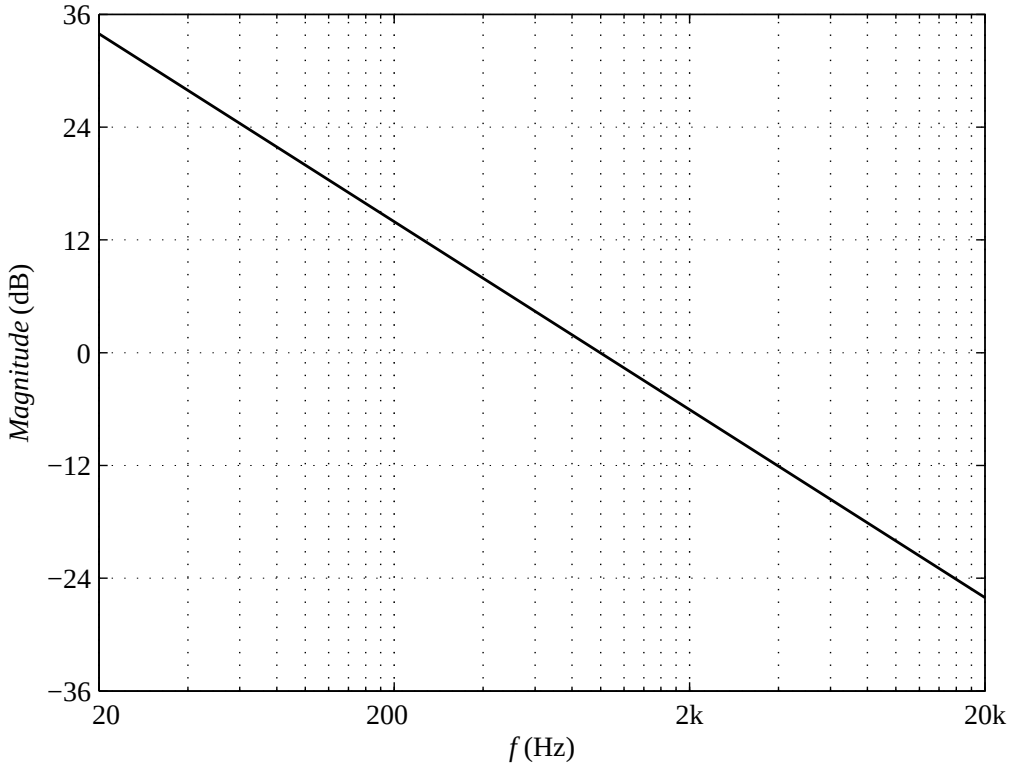

Figure 7: Ideal integration characteristic.

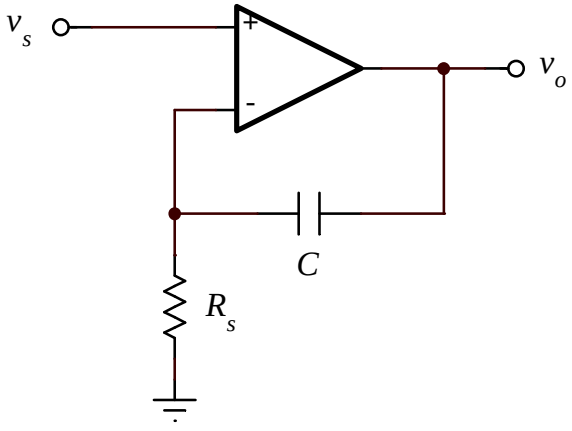

Figure 8: Voltage integrator.

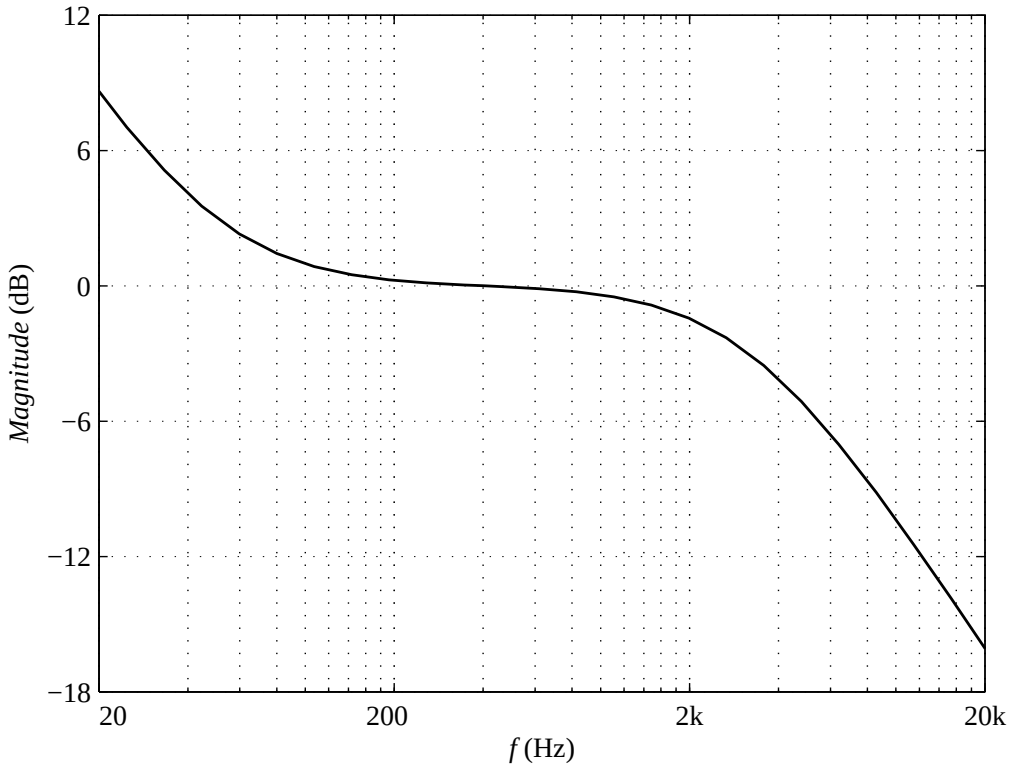

Figure 9: NAB recording equalization, 7½ and 15 ips.

equalization schemes based upon the operating speed of the tape.

The NAB standard for recording at commercial tape speeds of 7½ and 15 inches-per-second (ips) is shown in Fig. 9. It consists of a first-order rise below 50 Hz, a zero-dB (flat) response between 50 and 3183 Hz, and a first-order attenuation beyond the 3183-Hz pole [13]. The original audio signal is subjected to this equalization prior to being physically recorded to tape. The NAB playback standard, as seen in Fig. 10, is the inverse of the recording equalization and must be applied upon playback for accurate reproduction of the original audio source. Zero-dB equalization is referenced to the net gain provided by the voltage amplifier.

When the NAB playback characteristic is combined with the effects of voltage integration described in Section 2.1.3, the overall response of the preamplifier stage

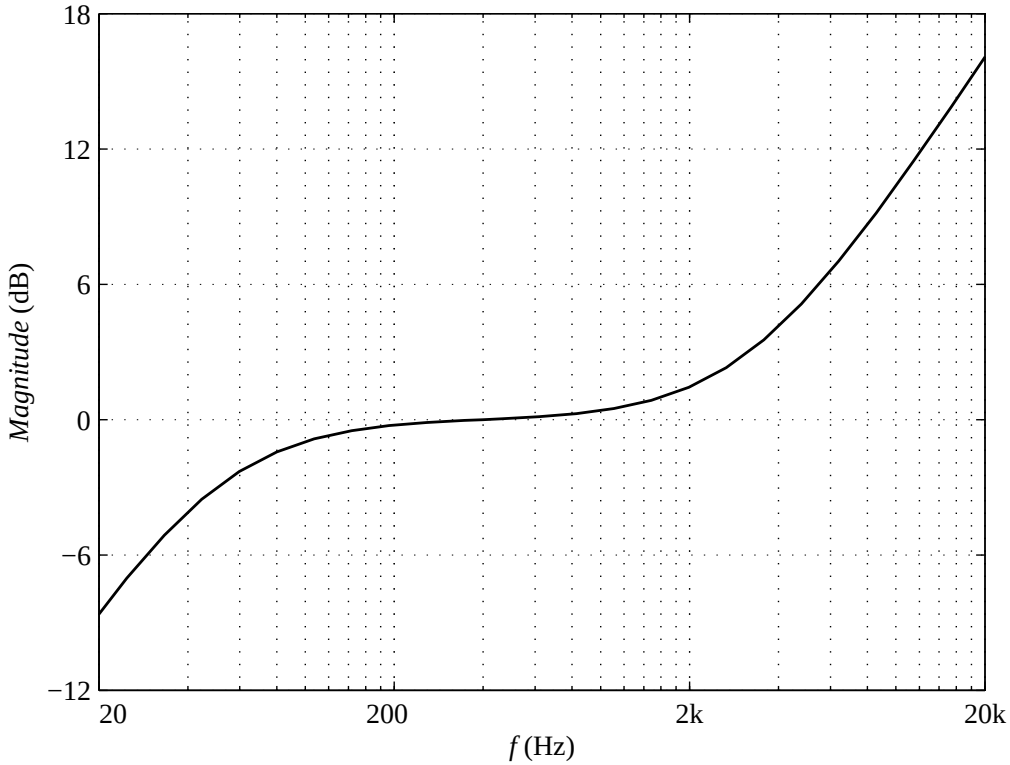

Figure 10: NAB playback equalization, 7½ and 15 ips.

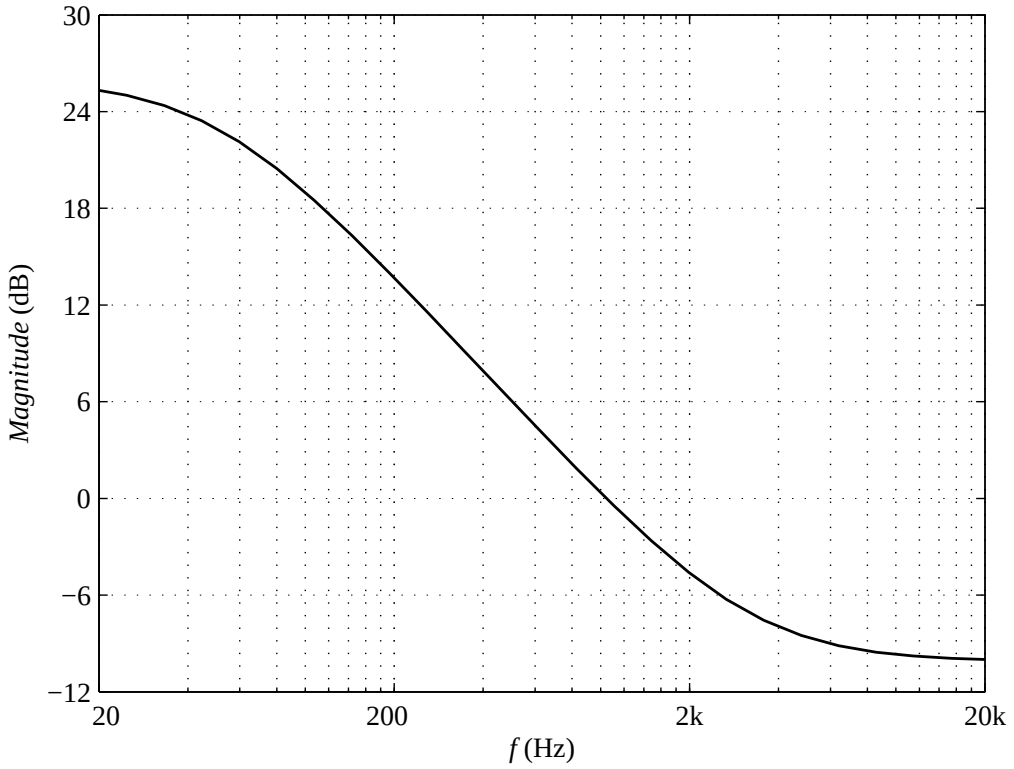

Figure 11: Effective equalization of playback preamplifier.

assumes the characteristic shown in Fig. 11; once again, 0 dB is referenced to the net gain of the amplifier. This response consists of a nominally-flat high-gain region below 50 Hz, a first-order attenuation from 50 to 3183 Hz, and a flat region of low gain from 3183 Hz onward. In practice, this equalization can be achieved by adding a resistor in parallel with the integrating capacitor to introduce a pole at 50 Hz; an additional series resistor is then placed in series within the feedback loop to cease voltage integration above 3183 Hz. Fig. 12 depicts an example of this approach. Correct playback equalization is therefore achieved while simultaneously compensating for the effects of $\frac{d\phi}{dt}$ and boosting the signal to a usable level.

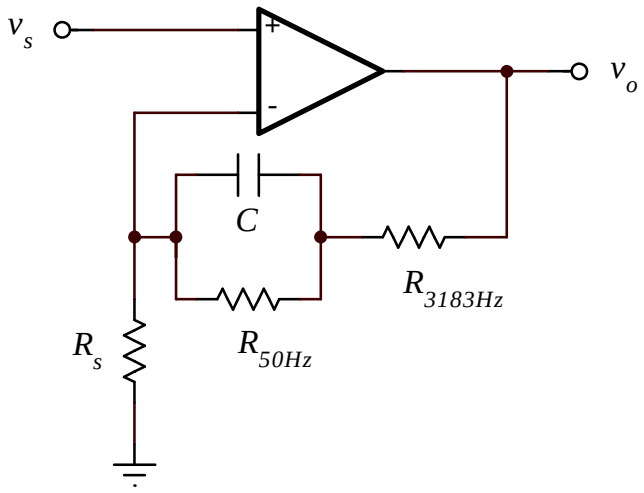

Figure 12: Voltage integrator with NAB playback equalization.

2.2 Drawbacks of Existing Designs

The basic topological approaches described in Section 2.1 have been in use since the 1950s [6]. Although the active devices used in playback circuitry have evolved from vacuum tubes to discrete transistors and integrated circuits, the basic methodology remains largely unchanged [9], [10], [11]. Existing playback preamplifiers employ a relatively complex equalization algorithm, integrating reproduce head voltage in addition to providing the required NAB equalization. Although complementary equalization characteristics theoretically "cancel out" to provide a linear response, undesired side effects can occur due to the imperfections of non-ideal active devices. Some potential detriments of added signal conditioning are discussed below.

2.2.1 Integration and Low-Frequency Distortion

Voltage integration is equivalent to a low-frequency boost, as seen in Fig. 7. Since the operation is performed as part of the amplifier's feedback loop, any distortion or anomaly introduced by the input of the preamplifier (that is, not present at the output of the reproduce head) will be susceptible to boost along with the desired tape

signal. The post-integration result is therefore greater distortion at lower frequencies, which can be especially harmful to audio fidelity [14].

2.2.2 NAB Equalization and High-Frequency Distortion

The NAB playback equalization curve of Fig. 10 is also introduced within the feedback loop of the preamplifier. In the same manner that voltage integration contributes to increased low-frequency distortion, the NAB playback characteristic can result in greater distortion at high frequencies due to the boost occurring above 3.183 kHz.

2.2.3 Spectral Discontinuity

Voltage integration and NAB equalization combine to form the transfer characteristic shown in Fig. 11; likewise, their respective contributions to distortion also combine. Frequency-dependent distortion, in particular that which occurs at levels *inversely* proportional to frequency, is referred to by Tritschler as *spectral discontinuity*. This manifests as audible buzzing or "muddiness" in the low-end and harsh, "metallic" overtones in the high end [6]. Hiraga also notes that this phenomenon is easily discernable by the human ear and, as such, should be avoided even if overall total harmonic distortion (THD) is relatively low. For example, an amplifier with a measured THD of 0.1% at 1 kHz and 1% at 100 Hz would exhibit less perceived fidelity than an amplifier with a THD of 1.5% for all test frequencies [14].

3 Proposed Solution - The Transresistance Amplifier

The main drawbacks of existing playback preamplifiers derive from the amount of spectral manipulation involved. Accordingly, the elimination of voltage integration and/or the NAB transfer curve is key to improving performance. NAB equalization is required due to the limitations of the medium itself and is set by industry standards; hence it is not a design variable within the scope of this research. Integration, however, is necessitated solely by the preamplifier topology, which is driven by a voltage signal $v_s(t)$ not directly proportional to the magnetic flux $\phi(t)$ of the tape. The proposed solution is therefore to employ a different topology driven by flux-proportional reproduce head current $i_s(t)$ instead of voltage. The need for integration is eliminated, thus minimizing the adverse effects of equalization.

3.1 Reproduce Head Current

The inductive properties of the reproduce head shown in Fig. 4 allow the voltage across its terminals to be expressed as

$$v_s(t) = L_s \frac{di_s(t)}{dt} \tag{3.1}$$

where L_s is the inductance of the head and $\frac{di_s(t)}{dt}$ is the rate of change of the winding current with respect to time. If (3.1) is combined with (2.1) and both are sides integrated with respect to time, an expression for the winding current of the reproduce head is obtained:

$$i_s(t) = \frac{N}{L_s}\phi(t). \tag{3.2}$$

As can be seen, $i_s(t)$ is directly proportional to $\phi(t)$, making the winding current a desirable input signal for the playback preamplifier if maximum fidelity is to be preserved.

3.2 Background of the Current-Driven Approach

Boegli was among the first to indirectly propose an alternate method for tape playback preamplification, describing a scenario in which an *anode follower* is used to amplify the output current of the reproduce head [4]. The anode follower is simply any inverting gain element with shunt-shunt negative feedback applied. This topology features a very low input impedance, enabling it to be driven by the head's relatively small output current rather than voltage.

Several years later, Perandi described the use of a *transimpedance amplifier* as a playback preamplifier for phonograph cartridges [5]. From an electronic standpoint, the playback process for a phonograph cartridge is identical to that of magnetic tape, albeit with a different equalization standard [8]. Transimpedance, also referred to as *transresistance*, is simply the controlled ratio of output voltage v_{out} to input current i_{in} of a system and is given by

$$r_m = \frac{v_{out}}{i_{in}}. \tag{3.3}$$

An ideal transresistance amplifier is a current-controlled voltage source where r_m is a constant greater than 1. This theoretically enables the linear conversion of input current to an amplified output voltage. Boegli's anode follower acts as a practical transresistance amplifier when driven by a current source. Perandi's design is likewise based on a practical transresistance amplifier implemented via a novel vacuum tube-MOSFET hybrid topology.

The concept suggested by Boegli and Perandi was later expanded upon by Tritschler, who presented a transresistance amplifier design specifically for analog tape play-

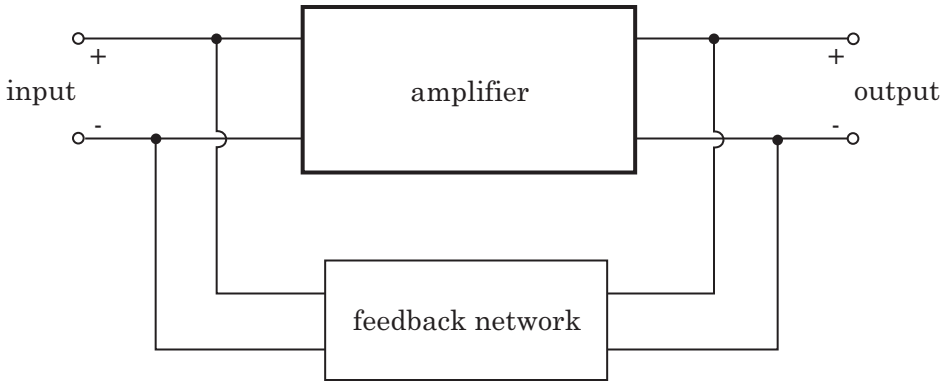

Figure 13: Shunt-shunt feedback.

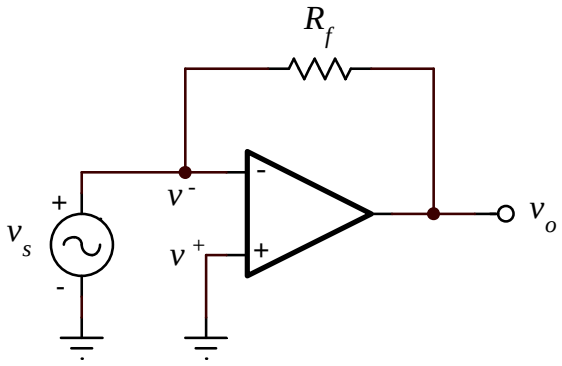

Figure 14: Standard inverting op-amp configuration.

back applications [6]. As opposed to a multi-stage discrete valve or transistor design, Tritschler takes advantage of the high-gain, low-noise properties of modern integrated circuits by adopting a dual op-amp approach. It is this topology that will form the basis for the design proposed herein.

3.3 Theory of the Op-Amp -Based Transresistance Amplifier

The transresistance amplifier is based upon the standard shunt-shunt negative feedback topology shown in Fig. 13. The equivalent circuit of an operational amplifier with shunt-shunt negative feedback is the standard inverting configuration seen in Fig. 14. If the voltage source v_s is replaced with a current source i_s, the circuit may

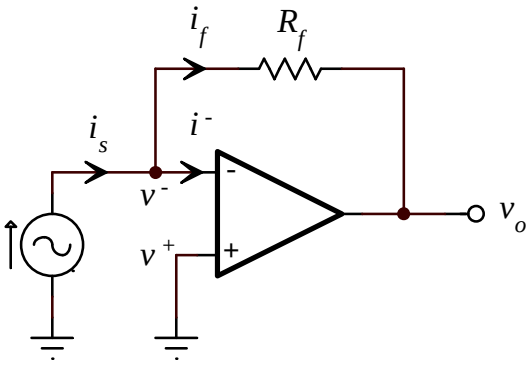

Figure 15: Inverting op-amp driven by current source.

be redrawn as shown in Fig. 15. This circuit forms the basic topology of the transresistance amplifier. A general transfer function may be derived by assuming the op-amp is *approximately* ideal. Ideal op-amp properties dictate that

$$v^- \cong v^+ \tag{3.4}$$

and

$$i^- \cong 0 \tag{3.5}$$

where v^- and v^+ are the inverting and non-inverting input voltages, respectively, and i^- is the inverting input current. Ohm's Law and Kirchoff's Voltage Law state that

$$v^- - v_o = i_f R_f \tag{3.6}$$

where v_o is the output voltage of the amplifier and i_f is the current through the feedback resistor R_f. In this topology, the non-inverting input is connected to ground; it is therefore clear from (3.4) that

$$v^- \cong 0. \tag{3.7}$$

Likewise, from (3.5) and Kirchoff's Current Law, it follows that

$$i_f \cong i_s. \tag{3.8}$$

Substituting (3.7) and (3.8) into (3.6), the output voltage is given by

$$-v_o \cong i_s R_f. \tag{3.9}$$

Feedback resistance may therefore be expressed in terms of output voltage and input current as

$$R_f \cong \left| \frac{v_o}{i_s} \right|. \tag{3.10}$$

It is apparent from (3.3) and (3.10) that the transresistance of a current-driven inverting op-amp is simply the value of R_f in ohms. In terms of magnetic tape playback preamplification, this topology represents a linear means of converting the small current generated by the reproduce head to an amplified voltage signal.

4 Analysis, Design, and Simulation

4.1 Design Procedure

The transresistance amplifier topology is based on shunt-shunt negative feedback, which may be implemented via any one of the following methods:

- Discrete vacuum tubes
- Discrete transistors
- Vacuum tube-transistor hybrids
- Integrated circuit op-amps

Boegli [4] offers various discrete tube and transistor designs that pre-date integrated circuits, while Perandi [5] proposes an intricate hybrid circuit. However, Tritschler's transresistance preamplifier consists of a dual op-amp and minimal passive components, while theoretically offering the same performance enhancements as other variants [6]. The added benefit of a smaller, less expensive circuit is an important design factor for mass-produced consumer electronics. It is therefore the dual inverting op-amp configuration that will form the basis for the transresistance preamplifier presented herein.

4.1.1 Transresistance Stage

The basic topology of the op-amp transresistance amplifier is as shown in Fig. 15, i.e., an inverting configuration driven by a current source. The reproduce head itself is not an ideal current source, but may be modeled via an ideal small-signal current

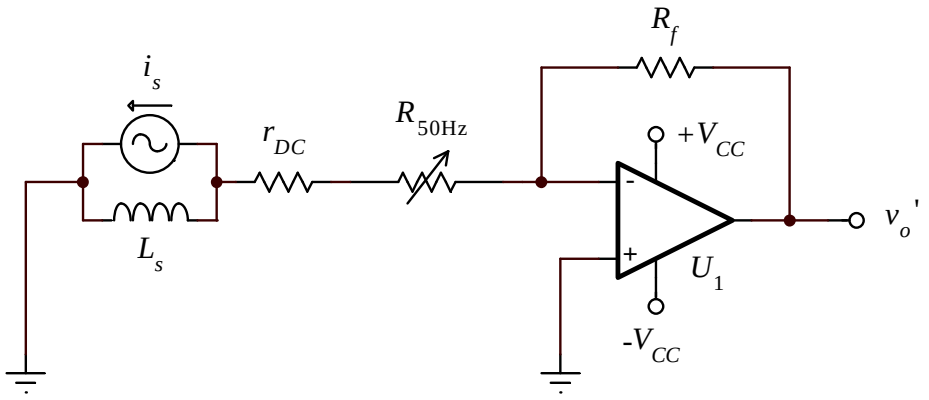

Figure 16: Transresistance stage of playback preamplifier.

source i_s in parallel with the nominal inductance of the head L_s, connected in series to the nominal DC resistance of the head r_{DC} as shown in Fig. 16. Given the narrow bandwidth of audio applications, the parasitic capacitance of the head is assumed to be sufficiently small enough that it may be neglected. Note that the polarity of the reproduce head has been reversed such that it operates as a *negative current source*. This is done to ensure that the output voltage of the inverting amplifier is positive with respect to the original voltage signal recorded to tape. The magnetic flux of the tape surface possesses an absolute polarity reflected by the current and, as such, polarity reversal is simply a matter of wiring the reproduce head "backwards."

Since the shunt-shunt negative feedback topology of this amplifier renders the inverting input a virtual ground per (3.7), the series combination of L_s and r_{DC} forms a first-order RL high-pass filter at the input. This contributes a pole of frequency f_{in} given by

$$f_{in} = \frac{r_{DC}}{2\pi L_s}. \tag{4.1}$$

Recalling the 50-Hz pole required by NAB equalization upon playback, it is clear that the reproduce head itself will provide this equalization if properly selected. The

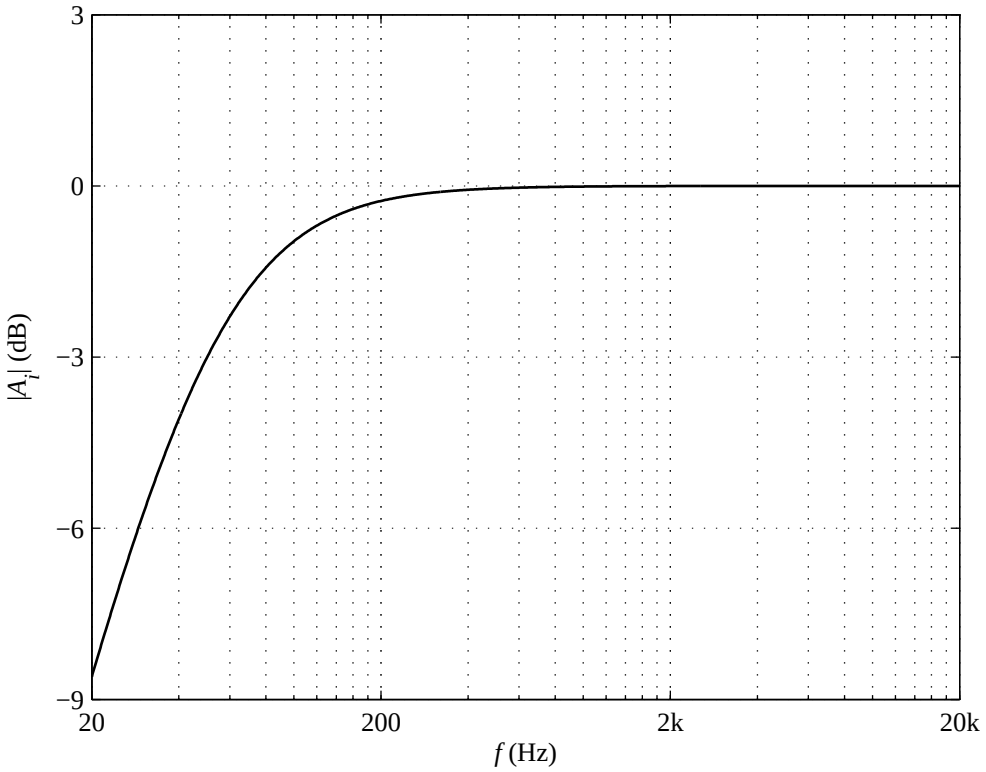

Figure 17: Response of reproduce head operated as a current source, $\frac{r_{DC}}{L_s} = 100\pi$.

designer must therefore choose a reproduce head that meets the condition

$$\frac{r_{DC}}{2\pi L_s} = 50\,\text{Hz}$$

i.e.,

$$\frac{r_{DC}}{L_s} = 100\pi. \tag{4.2}$$

The desired transfer characteristic of the reproduce head operated as a current source is shown in Fig. (17). DC resistance and nominal inductance are specifications provided by the manufacturer; the ratio $\frac{r_{DC}}{L_s}$ generally varies by reproduce head type and/or grade [7]. In order to allow $\pm 5\%$ compensation for any likely variation in actual head inductance, DC resistance and/or tape calibration, a head with a DC

resistance $r_{DC}^{'}$ of approximately 95% the value nominally required is selected. A potentiometer R_{50Hz} of at least 10% the nominal DC resistance is then added in series. This allows the effective r_{DC} to be adjusted higher or lower as needed, i.e.,

$$r_{DC}^{'} \leq r_{DC} \leq r_{DC}^{'} + R_{50Hz}$$

$$0.95 r_{DC} \leq r_{DC} \leq 1.05 r_{DC}. \tag{4.3}$$

The individual design guidelines are therefore

$$r_{DC}^{'} \cong 95\pi L_s \tag{4.4}$$

and

$$R_{50Hz} \geq 10\pi L_s. \tag{4.5}$$

The variable resistor should be set to a nominal value of

$$R_{50Hz}^{'} = r_{DC} - r_{DC}^{'}$$

$$= 100\pi L_s - r_{DC}^{'}. \tag{4.6}$$

The value of the feedback resistor R_f is equal to the desired current-to-voltage gain, as established by (3.10). Typically, the preamplifier is designed to provide a specified output voltage v_o sufficient to drive a line-level amplifier. Nominal maximum output voltage of the head $v_{s(rms)}$ is provided by the manufacturer in V(rms) at some frequency f_s (typically 1 kHz), and can be converted to an equivalent maximum constant-current output level $i_{s(rms)}$. If the time-varying output voltage of the head is given by

$$v_s(t) = V_{peak} \sin(2\pi f_s t)$$

$$= \frac{v_{s(rms)}}{\sqrt{2}} \sin(2\pi f_s t) \tag{4.7}$$

then the differential component of (3.1) implies that the time-varying output current is of the form

$$i_s(t) = -I_{peak} \cos(2\pi f_s t)$$

$$= -\frac{i_{s(rms)}}{\sqrt{2}} \cos(2\pi f_s t). \tag{4.8}$$

Substituting these conditions into (3.1) gives

$$\frac{v_{s(rms)}}{\sqrt{2}} \sin(2\pi f_s t) = L_s \frac{d\left[-\frac{i_{s(rms)}}{\sqrt{2}} \cos(2\pi f_s t)\right]}{dt}$$

$$= -\frac{2\pi f_s L_s i_{s(rms)}}{\sqrt{2}} \left[-\sin(2\pi f_s t)\right]$$

$$= \frac{2\pi f_s L_s i_{s(rms)}}{\sqrt{2}} \sin(2\pi f_s t) \tag{4.9}$$

and rearranging (4.9) reveals

$$i_{s(rms)} = \frac{v_{s(rms)}}{2\pi f_s L_s}. \tag{4.10}$$

From (3.10) and (4.10), the design equation for the feedback resistor is therefore

$$R_f = \frac{2\pi f_s L_s v_{o(rms)}}{v_{s(rms)}} \tag{4.11}$$

where $v_{o(rms)}$ is the desired output voltage of the preamplifier in V(rms).

4.1.2 High-Frequency Boost Stage

Adherence to the NAB equalization standard dictates that, in addition to attenuation below 50 Hz, playback must also provide a first-order rise starting at 3.183 kHz. Accomplishing this within the transresistance stage would require a high-pass RL

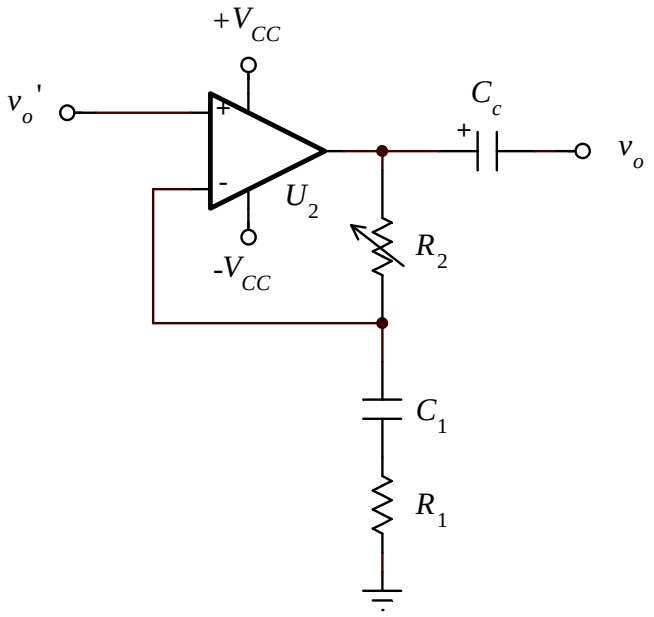

Figure 18: High-frequency boost stage of playback preamplifier.

shelving filter with an impractically large inductor, due to the high midband gain. Therefore, a second gain stage is needed to provide the high-frequency boost, as depicted in Fig. 18.

This stage is implemented via a standard non-inverting op-amp since the voltage output of the transresistance stage is non-inverted with respect to the magnetic flux of the tape. Series-shunt negative feedback allows for the use of a capacitive, rather than inductive, network to boost the gain at desired frequencies. Since the transfer function of the circuit in Fig. 18 can be expressed in terms of capacitive reactance X_{C_1}, i.e.,

$$\begin{aligned} A_v(f) &\cong 1 + \frac{R_2}{R_1 + |X_{C_1}|} \\ &\cong 1 + \frac{R_2}{R_1 + \frac{1}{2\pi f C_1}} \end{aligned} \tag{4.12}$$

the feedback network acts as a shelved high-pass filter with cutoff frequencies

$$f_{H1} = \frac{1}{2\pi\left(R_1 + R_2\right)C_1} \tag{4.13}$$

$$f_{H2} = \frac{1}{2\pi R_1 C_1} \tag{4.14}$$

and shelving gains

$$A_{v1} \cong 1 \tag{4.15}$$

$$A_{v2} \cong 1 + \frac{R_2}{R_1}. \tag{4.16}$$

Since inaudible high frequencies have been shown to play a key role in audible fidelity, particularly in terms of harmonic masking [14], the upper shelving cutoff frequency f_{H2} should be chosen such that the boost is maintained well beyond the upper range of the audio spectrum, i.e.,

$$f_{H2} \geq 10\, f_{audible\,(max)}$$

$$f_{H2} \geq 10 \times 20,000\,\mathrm{Hz}$$

$$f_{H2} \geq 200\,\mathrm{kHz}. \tag{4.17}$$

Therefore, from (4.14),

$$R_1 C_1 \leq \frac{2.5 \times 10^{-6}}{\pi}. \tag{4.18}$$

The lower shelving frequency f_{H1} is equivalent to the boost frequency. As with the low-frequency cutoff of the first stage, the second stage should provide for some degree of adjustment to f_{H1}; this is often necessary due to component tolerances and/or calibration. Hence either R_1 or R_2 must be a variable resistor. Provided R_1 has been properly selected per (4.14), feedback resistor R_2 affects only f_{H1} and is the preferred adjustment. To allow for a $\pm 10\%$ compensation adjustment to the high

frequency zero, (4.13) is rearranged as

$$R_2 = \frac{1}{2\pi f_{H1} C_1} - R_1 \tag{4.19}$$

and 90% of the desired 3.183-kHz boost frequency is substituted, yielding

$$R_{2(max)} \geq \frac{1}{2\pi \left(0.9 f_{H1}\right) C_1} - R_1$$

$$R_{2(max)} \geq \frac{1}{2\pi \left(0.9 \times 3183\right) C_1} - R_1$$

$$R_{2(max)} \geq \frac{0.0001745}{\pi C_1} - R_1. \tag{4.20}$$

From (4.19), the potentiometer should therefore be set to a nominal resistance of

$$R_2^{'} = \frac{0.0001571}{\pi C_1} - R_1. \tag{4.21}$$

As long as the conditions of (4.18) are satisfied, the upper shelf gain given by (4.16) is not a design factor. Additionally, (4.15) demonstrates that below 3.183 kHz the second stage merely acts as a non-inverting buffer, preserving the gain and low-frequency NAB equalization of the first stage.

The decoupling capacitor C_c is present to remove any DC offset voltage prior to the line-level amplifier, and is also a safeguard against DC circuit faults. As this capacitor introduces an additional low-frequency pole f_{C_c}, it must be selected with the system's low frequency response in mind. The effect of C_c is given by

$$f_{C_c} = \frac{1}{2\pi R_{load} C_c} \tag{4.22}$$

where R_{load} is the load seen by the playback preamplifier. Since non-ideal, high-quality reproduce heads are nominally limited to 25 Hz as a minimum operating

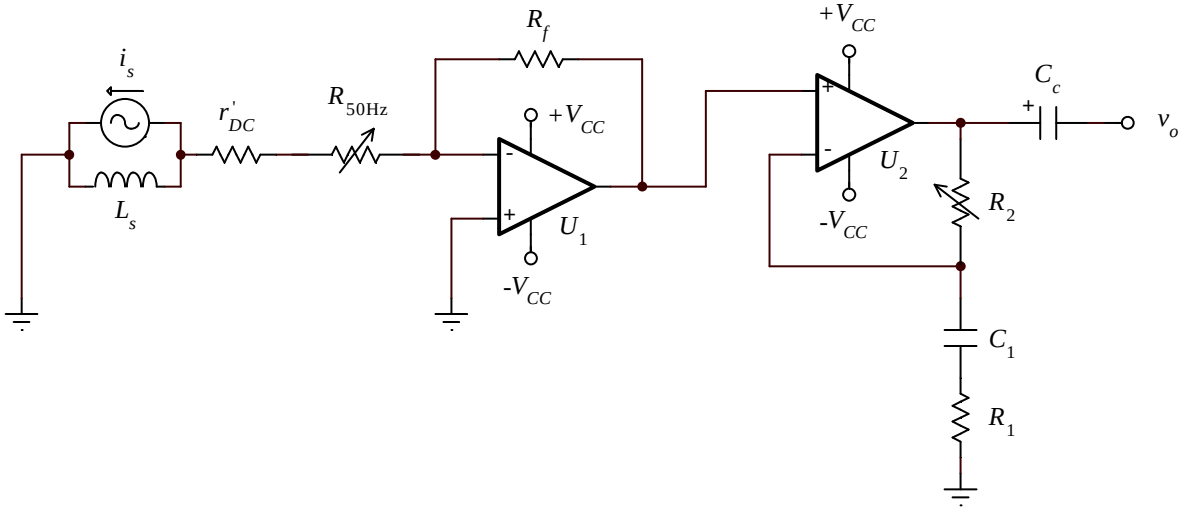

Figure 19: Transresistance playback preamplifier schematic.

frequency [7], the condition

$$f_{C_c} \leq \frac{1}{5} f_{(min)}$$

$$f_{C_c} \leq \frac{25\,\text{Hz}}{5}$$

$$f_{C_c} \leq 5\,\text{Hz}$$

is sufficient. Therefore, (4.22) may be rewritten as

$$C_c \geq \frac{1}{10\pi R_{load}}. \tag{4.23}$$

Assuming the output of the preamplifier is sub-line level, i.e., less than 200 mV(rms), then the peak-to-peak voltage across C_c is well under 1 V. Voltage stresses are therefore negligible and an inexpensive, low-voltage capacitor may be used.

4.1.3 Design Calculations

The complete playback preamplifier circuit is seen in Fig. 19. First and foremost, the proper reproduce head must be selected based on inductance and DC resistance.

Most reproduce heads range from 100 to 600 mH [7]; nominal inductance is thus selected as

$$L_s = 400\,\text{mH}.$$

From (4.4), the required DC resistance is

$$r'_{DC} \cong 95\pi \times 0.4$$

$$\cong 119.4$$

$$= 120\,\Omega.$$

Likewise, the low-frequency biasing potentiometer is

$$R_{50\text{Hz}} \geq 10\pi \times 0.4$$

$$R_{50\text{Hz}} \geq 12.6$$

$$= 50\,\Omega.$$

From (4.6) the variable resistor should be set to a value of

$$R'_{50\text{Hz}} = (100\pi \times 0.4) - 120$$

$$= 5.664\,\Omega.$$

No manufacturer specifications were available for a 400-mH / 120-Ω reproduce head; this head would likely have to be custom-manufactured for mass production. However, two closely-rated reproduce heads are the Nortronics WP-B1HY7K (L_s = 400 mH, r_{DC} = 140 Ω, $v_{s(rms)}$ = 2.0 mV at 1 kHz) and PR-B2H7K (L_s = 400 mH, r_{DC} = 200 Ω, $v_{s(rms)}$ = 3 mV at 1 kHz). The difference in output voltage between

these similar heads allows the output voltage of the required reproduce head to be linearly interpolated as $v_{s(rms)} \cong 1.7\,\text{mV}$.

In order to minimize noise, subsequent line-level amplification stages require a nominal input of at least 100 mV(rms) [8], [6]. Playback preamplifier output is therefore selected as $v_{o(rms)} = 150\,\text{mV}$ for this design. From (4.11) the required feedback transresistance is

$$R_f = \frac{2\pi \times 1000 \times 0.4 \times 0.15}{0.0017}$$

$$= 221,759.48$$

$$\cong 220\,\text{k}\Omega.$$

As the transresistance amplifier is capable of very large current-to-voltage gains with high linearity, R_f may be easily adjusted to account for any reasonable discrepancy between the estimated and actual values of $v_{s(rms)}$.

The shunt RC network in the second stage's feedback loop is now determined via (4.18). Selecting

$$C_1 = 4.7\,\text{nF}$$

gives

$$R_1\left(4.7 \times 10^{-9}\right) \leq \frac{2.5 \times 10^{-6}}{\pi}$$

$$\leq 169.3\,\Omega$$

$$= 140\,\Omega.$$

Therefore, from (4.20),

$$R_{2(max)} \geq \frac{0.0001745}{\pi\left(4.7 \times 10^{-9}\right)} - 140$$

$$R_{2(max)} \geq 11,678.1\,\Omega$$

and the feedback potentiometer is selected as

$$R_2 = 20\,\mathrm{k}\Omega.$$

From (4.21), this variable resistor should be set to

$$R_2' = \frac{0.0001571}{\pi\,(4.7 \times 10^{-9})} - 140$$

$$= 10,499.7\,\Omega.$$

Assuming $R_{load} \cong 5\,\mathrm{k}\Omega$, that is, the input resistance of the line-level amplifier is approximately 5 kΩ, the output coupling capacitor is selected via (4.23) as

$$C_c \geq \frac{1}{10\pi\,(5000)}$$

$$\geq 6.366 \times 10^{-6}$$

$$= 10\,\mu\mathrm{F}.$$

In practice, all fixed resistors should be low-noise metal film type, 1/4-watt, 2% tolerance or less. Variable resistors should be low-noise sealed conductive plastic. Potentiometer $R_{50\mathrm{Hz}}$ should be linear taper, while R_2 should be logarithmic in order to balance sensitivity when calibrating for frequency response. The high-frequency boost capacitor C_1 should be polypropylene with a tolerance of 2.5% or less [15].

4.1.4 Op-Amp Selection and Supply Considerations

The NE5534 operational amplifier is selected as the active device for both stages of the preamplifier. This inexpensive op-amp has very low THD across the audio spectrum, and its low input voltage noise and high unity-gain bandwidth are particularly beneficial in the transresistance stage of the preamplifier. Simulated performance is,

in fact, found to be comparable to that of specialty audio op-amps costing nearly 20 times more.

The NE5534 is *uncompensated*; it is internally compensated only for a gain of 3 or greater, with pins provided to add an external compensation capacitor if necessary. Uncompensated op-amps offer greater bandwidth but are less stable at high frequencies. They are therefore ideal for use in high-gain, low-frequency applications since the additional bandwidth can be traded for greater gain and linearity at frequencies where stability is not an issue [16]. This makes the NE5534 well-suited to the initial transresistance stage without the use of additional compensation. It is also suitable for use in the second stage as it requires less gain but slightly more bandwidth to extend the high-frequency boost to 200 kHz. This tradeoff preserves stability even though second stage gain is less than 3 for frequencies under 3.183 kHz.

Like most modern op-amps, the NE5534 will operate under DC supply conditions as low as ± 5 V. Since the peak output voltage of the preamplifier is given by

$$v_{o(peak)} = v_{o(rms)} \times \sqrt{2}$$

$$= 0.15\sqrt{2}$$

$$= 212.13\,\text{mV}$$

and is far less than typical $V_{CC} - V_{sat}$, supply rails of

$$\pm V_{CC} = \pm 5\,V_{DC}$$

may be used.

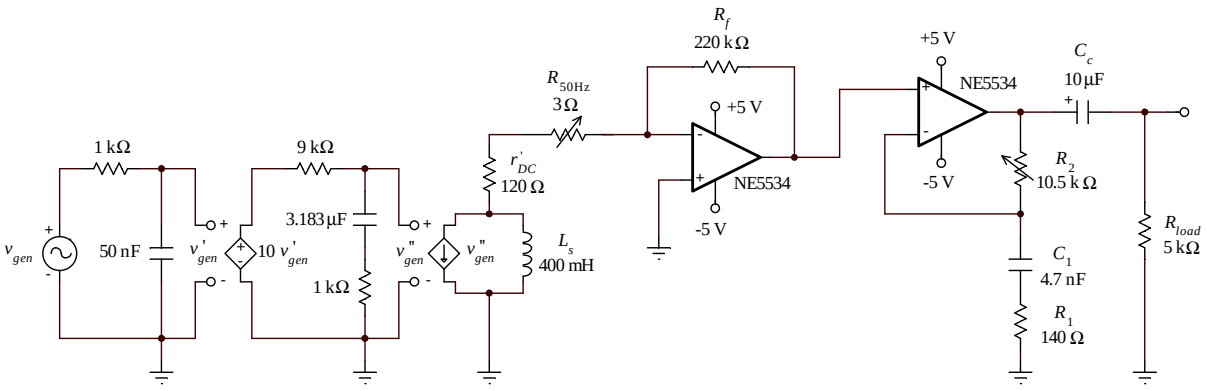

Figure 20: Simulated transresistance playback preamplifier circuit.

4.2 SPICE Simulation

4.2.1 Frequency, Transient, and Fourier Analyses

The transresistance playback amplifier is generated in SPICE as shown in Fig. 20, based upon the design considerations in Sections 4.1.3 and 4.1.4. The purpose of the playback preamplifier is to reproduce a signal that is linear with respect to the original audio source; however, the output is not linear with respect to the input signal of the circuit. In order to reconcile this apparent contradiction between high-fidelity and nonlinear amplification, and also to provide results that are easily analyzed in the context of linearity, a source is modeled to represent actual input current i_s as shown in Fig. 21. Recalling that the flux-proportional signal on tape has the transfer characteristic shown in Fig. 9, i_s provided by the ideal current source in Fig. 16 must possess the same frequency response. This zero-dB reference level of this response is equal to the nominal output current of the head given by (4.10). This is implemented via the network depicted in Fig. 21, consisting of:

- a small signal voltage source v_{gen}
- a first-order low-pass filter, $f_c = 3.183$ kHz
- a voltage-controlled voltage source v'_{gen}

- a first-order low-pass shelving filter, $f_1 = 5\,\text{Hz}$ and $f_2 = 50\,\text{Hz}$
- a voltage-controlled current source v''_{gen}

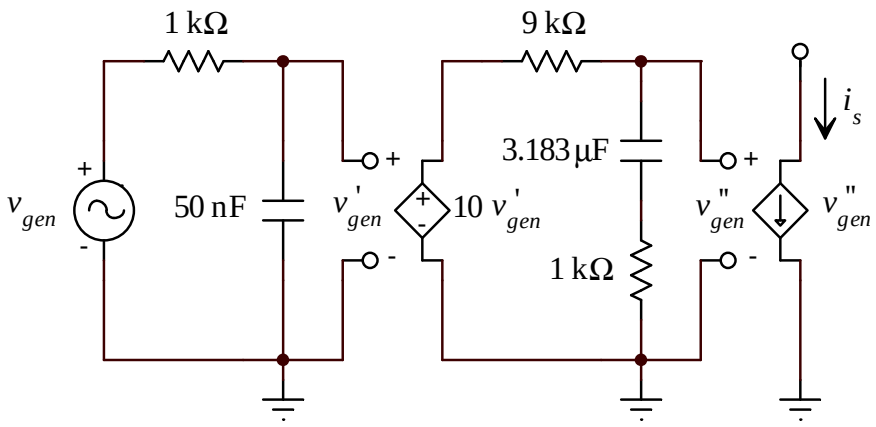

Figure 21: Model of reverse-polarity reproduce head current source.

Source v_{gen} provides a voltage signal that is easily shaped by passive filtering. This voltage is set to the same magnitude, frequency, and shape as the desired reproduce head current i_s. The first-order low-pass filter provides the same high-frequency cutoff as the NAB recording characteristic. Dependent source v'_{gen} supplies 20 dB of gain to counteract the 20-dB attenuation of the subsequent shelving filter. The shelving filter's components are selected to provide 20 dB of attenuation from 5 Hz to 50Hz. The gain provided by the dependent voltage source therefore simulates a rising response below 50 Hz. The output voltage of the shelving filter therefore possesses the ideal characteristic of reproduce head winding current, and is converted to the ideal current source i_s via a 1-to-1 dependent transfer. The simulated characteristic of the test source is shown in Fig. 22.

The full circuit in Fig. 20 also shows the actual values used for variable resistors $R_{50\text{Hz}}$ and R_2 to provide optimum simulated response. Resistance R_2 requires no adjustment from the value determined in Section 4.1.3. However, adjustment of $R_{50\text{Hz}}$

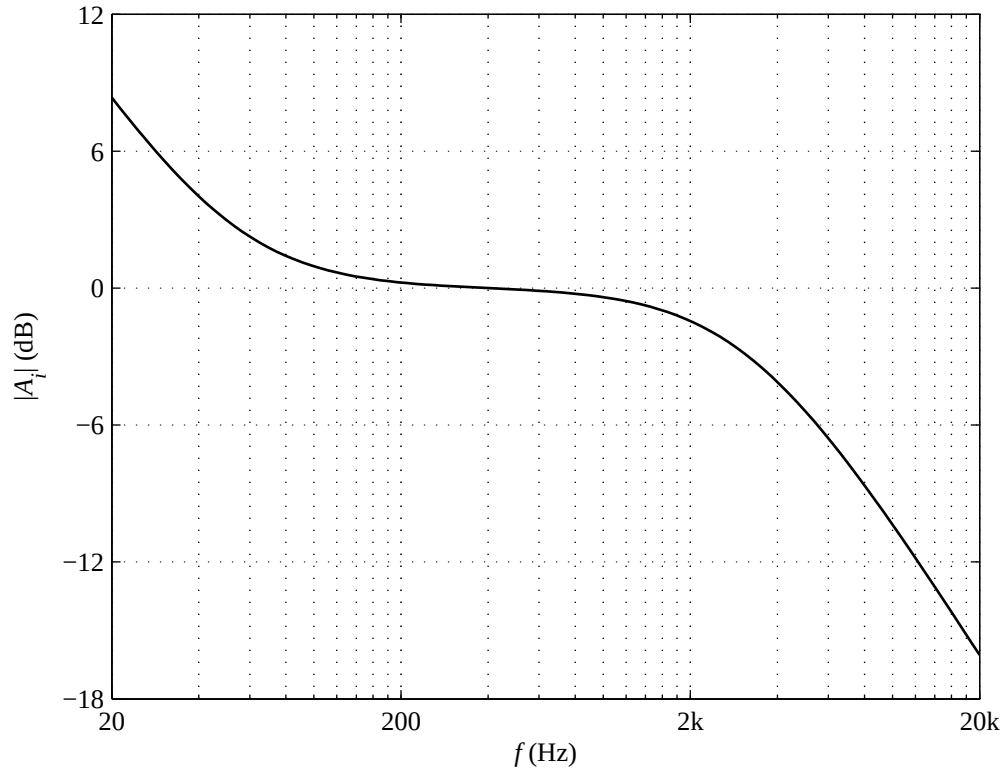

Figure 22: Simulated transfer characteristic of input current source model.

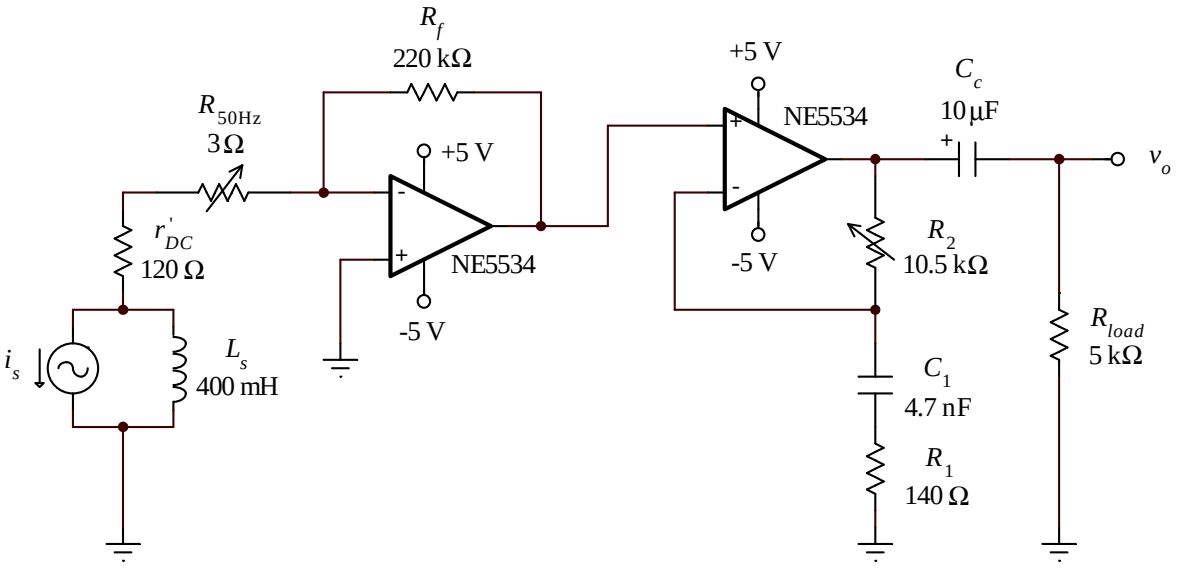

Figure 23: Simulated transresistance preamplifier circuit, source modified for noise analysis.

is necessary to place the low-frequency pole at exactly 50 Hz. Since the NE5534 model represents a non-ideal op-amp, the inverting input is not a perfect "virtual ground" and contributes additional impedance to the numerator of (4.1). This increases the low-frequency pole, which may be counteracted by decreasing $R_{50\text{Hz}}$.

4.2.2 Noise Analysis

Frequency-based noise analysis is performed to determine the amount contributed by the proposed transresistance preamplifier. For these purposes, use of the source model in Fig. 21 is not appropriate, as it models only *equalization* and not necessarily the *noise characteristic* of the signal on tape. Furthermore, the individual passive components in the source model each contribute noise not present in a real-world tape playback scenario. In order for the analysis to more accurately reflect noise contributed by the preamplifier itself, the source model is removed and replaced with an ideal current source as shown in Fig. 23.

4.2.3 Simulation Overview

All AC analysis is performed over the nominal audio bandwidth of 20 Hz to 20 kHz for the sake of clarity and comparison, with the exception of the extended bandwidth results displayed in Section 6.1. All transient analyses are run for a minimum of $\frac{100}{f}$ seconds to ensure steady-state output is reached. Time-varying voltage and current sources, where applicable, are set at a peak amplitude equal to the peak constant-current output of the reproduce head. From (4.10), this value is

$$\begin{aligned} i_{s(peak)} &= \sqrt{2} \times i_{s(rms)} \\ &= \frac{v_{s(rms)}\sqrt{2}}{2\pi f_s L_s} \\ &= \frac{0.0017\sqrt{2}}{2\pi(1000)(0.4)} \\ &= 0.957\,\mu\text{A}. \end{aligned} \tag{4.24}$$

Fourier series analysis is conducted for the 1st through 8th harmonics of a sine wave input with fundamental frequency f_o; sampling is initiated at $\frac{100}{f_o}$ seconds. For noise analysis, signal-to-noise ratio (SNR) calculations are referenced to the peak amplitude of the simulated output voltage at 400 Hz, i.e., the geometric mean of the low- and high-frequency NAB transition frequencies.

4.2.4 Frequency Response

The simulated magnitude and phase response of the playback preamplifier is shown in Figs. 24. The magnitude response is exceptionally flat, within ±0.34 dB across the audio spectrum. A midband gain of 106.84 dB is observed, which is nearly equal to the specified transresistance of the amplifier. Phase angle at 1 kHz is approximately 0.216° and deviates less than ±5° over the majority of the spectrum. A maximum angle of +23° is seen at 20 Hz.

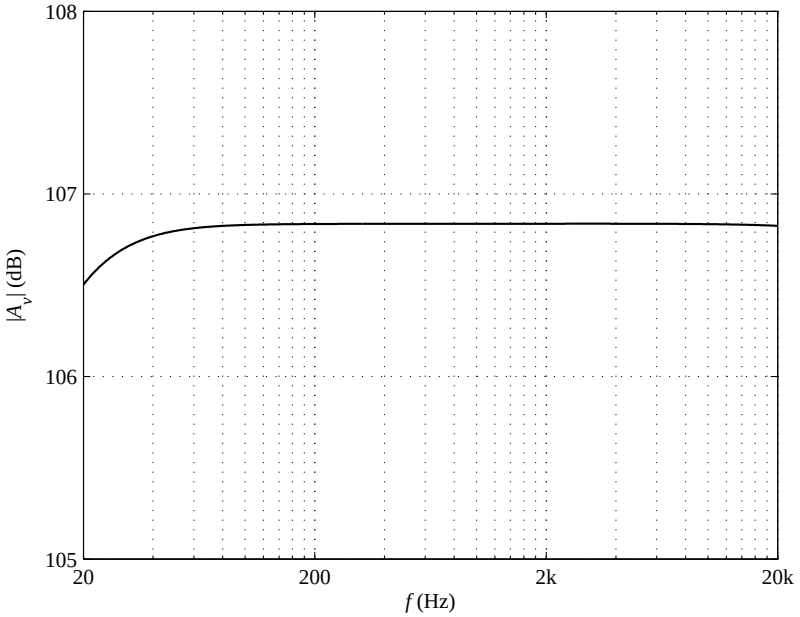

(a)

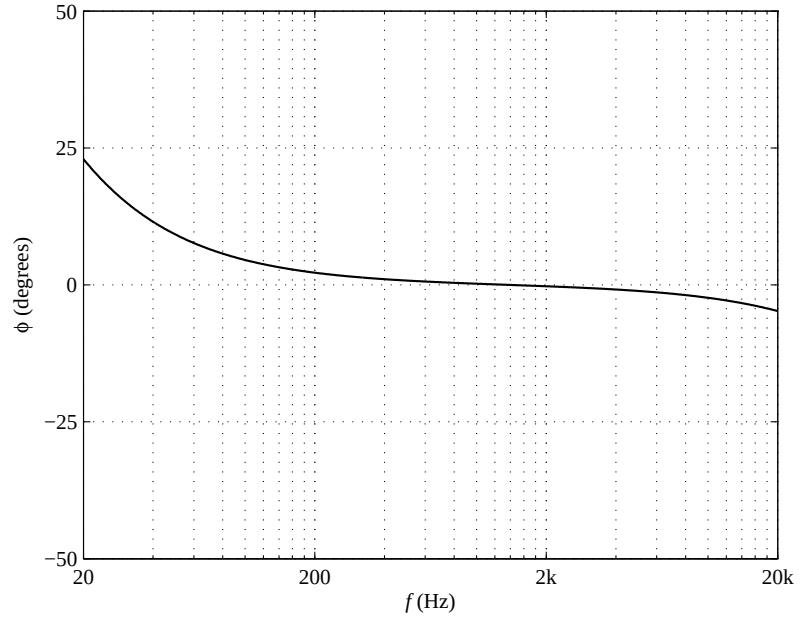

(b)

Figure 24: Simulated frequency response of transresistance playback preamplifier. (a) Magnitude. (b) Phase.

4.2.5 Transient Analysis

Fig. 25 shows the transient response of the preamplifier with standard audio test signals of a 1-kHz sine wave and a 20-kHz square wave. Peak voltage of the 1-kHz sine wave output is 209.88 mV, or 148.40 mV(rms), with a phase shift of approximately 0.23°. Square wave output at 20 kHz is slightly underdamped with a steady-state peak voltage 210.16 mV; overshoot is 6.7% with a rise time of 2.16 μs. Phase shift is −1.18°.

4.2.6 Spectral Analysis and THD

SPICE analysis provides for calculation of the Fourier series of the output based upon an input waveform of fundamental frequency f_{o}. Total harmonic distortion is then calculated as a ratio of the RMS voltage coefficients of the series [17], i.e.,

$$\mathrm{THD} = \left(\frac{\sqrt{v_{o(rms)2}^2 + v_{o(rms)3}^2 + ... + v_{o(rms)N}^2}}{v_{o(rms)1}} \right) \times 100\% \tag{4.25}$$

where $v_{o(rms)N}$ represents the RMS amplitude of the N^{th} harmonic of the fundamental ($N = 1$) frequency present at the output. However, graphical analysis of audio-frequency THD typically presents the individual coefficients of the Fourier series in dB rather than RMS voltage [14]. For the results presented below, all harmonics are referenced to the output level $v_{o(rms)1}$ of the fundamental tone.

Fig. 26 shows the harmonic spectrum of the proposed transresistance amplifier at 1 kHz, along with the corresponding SPICE calculation of THD.

The harmonic series displays a smooth, decreasing gradient, well under -120 dB from the fundamental. The simulated THD of 0.000082716% is exceptionally low.

The dynamic response of THD itself is of equal, if not greater, importance to overall fidelity as the singular value of THD at any one fundamental frequency [14]. For this reason, a sweep of several fundamental frequencies is performed to generate

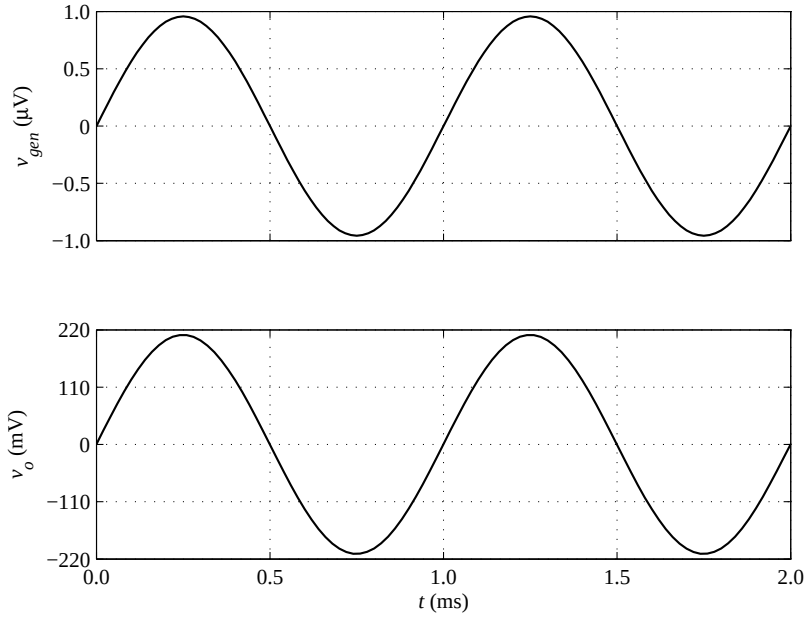

(a)

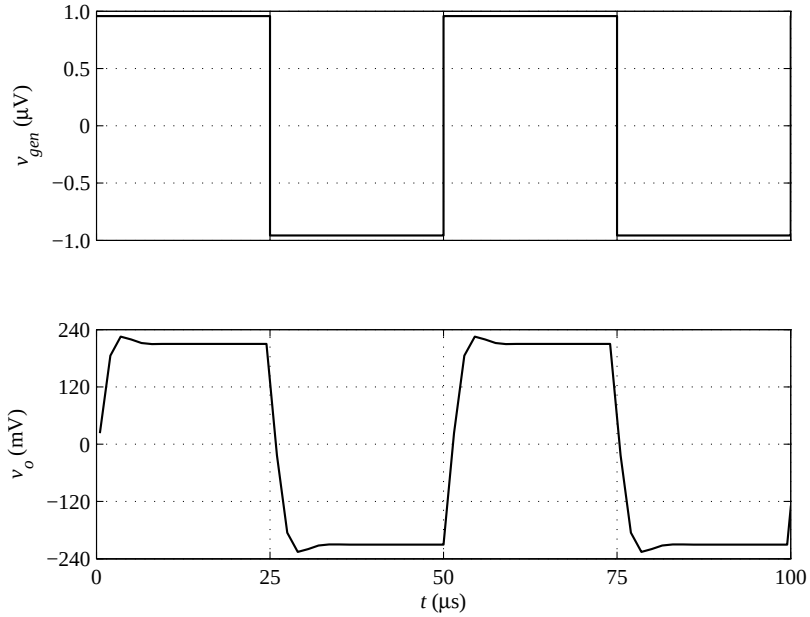

(b)

Figure 25: Simulated transient response of transresistance preamplifier. (a) 1-kHz sine wave input. (b) 20-kHz square wave input.

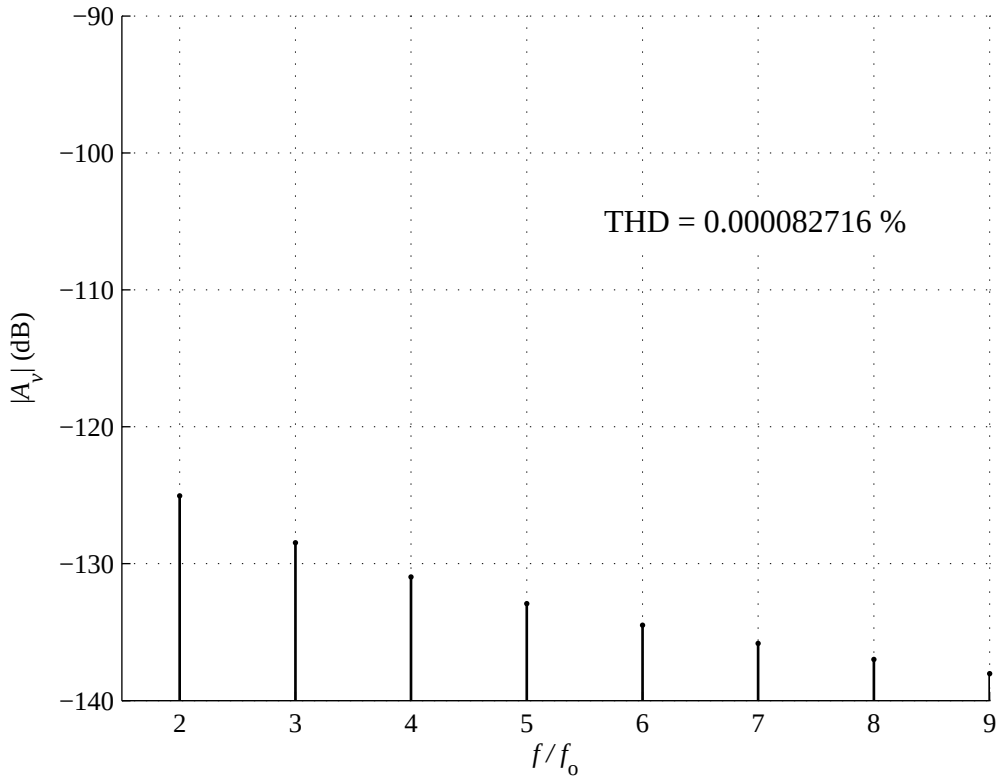

Figure 26: Harmonic spectrum and THD of simulated transresistance preamplifier, sine wave input, $f_o = 1$ kHz.

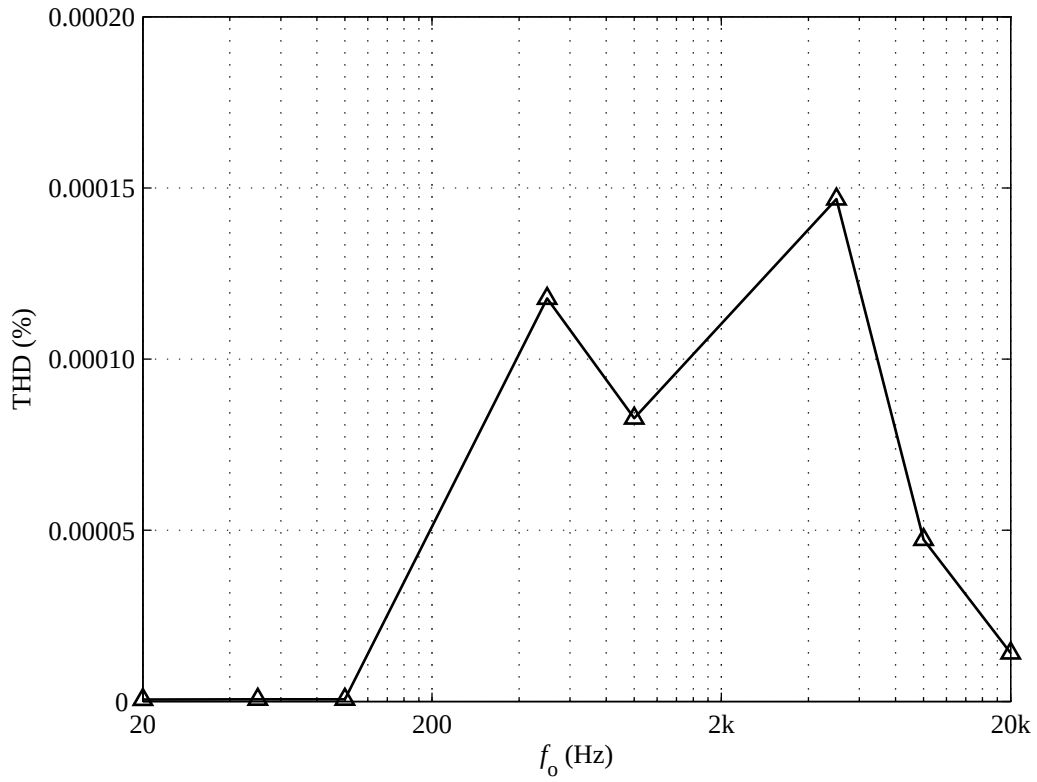

Figure 27: Effect of fundamental frequency f_o on THD of simulated transresistance preamplifier.

an approximate *THD spectrum*. The results are shown in Fig. 27. The calculated THD remains very low, i.e., less than 0.00015%, for all eight fundamental frequencies tested within the audio spectrum. More importantly, however, the response decreases with both frequency extremes, and is particularly flat at the low end.

4.2.7 Noise Analysis

The results of SPICE noise analysis are shown in Fig. 28. As can be seen, the SNR of the simulated amplifier is 65 dB or greater across the audio spectrum; midband SNR is approximately 68 dB. The shape of the curve likewise indicates that noise increases with frequency.

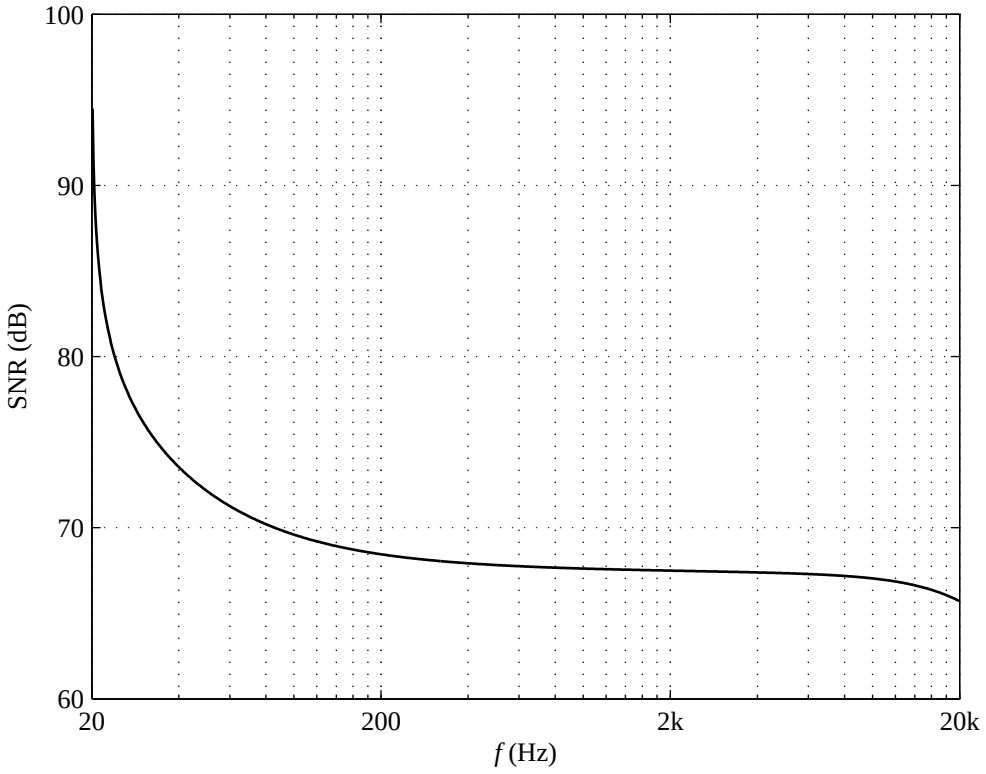

Figure 28: Noise analysis of simulated transresistance preamplifier.

5 Characterization of Existing Topologies

Quantification of the performance improvements provided by the transresistance preamplifier requires a comparative analysis of existing designs. Since no detailed evaluation of present technology was found in the literature search, two commercially-available playback preamplifier designs utilizing voltage integration are modeled and analyzed in SPICE. The original version of the transresistance preamplifier presented by Tritschler is also modeled and analyzed in order to validate a number of suggested design improvements.

5.1 Simulation

SPICE simulation is carried out using the same approach and parameters described in Section 4.2. For the sake of comparison to the proposed transresistance preamplifier, the gain of each existing design is normalized to obtain an output of approximately 150 mV(rms), or 106.84 dB of current-to-voltage gain using the same reproduce head. The source signal is provided by the same model used previously, albeit re-oriented for standard polarity as shown in the SPICE circuit of Fig. 29. This allows the output of each existing preamplifier to be directly compared to the proposed design, while still reflecting real-world operating conditions. Noise analysis likewise follows the same simulation approach as previously described. The circuit in Fig. 30 supplies the input to the simulated preamplifier for determining SNR.

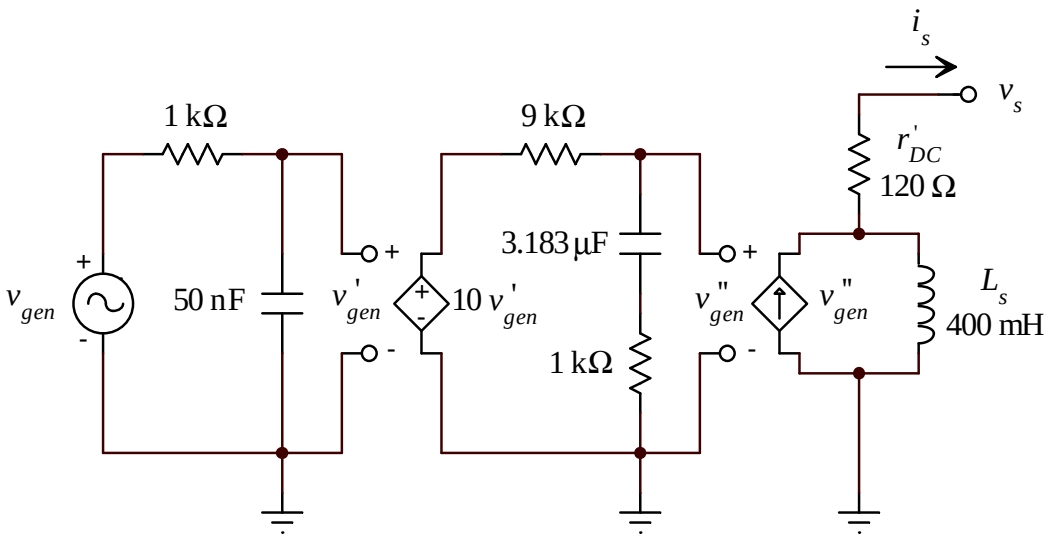

Figure 29: Simulated reproduce head source of standard polarity for frequency, transient, and Fourier analyses.

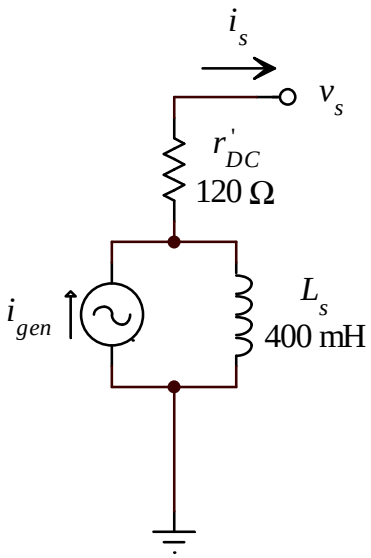

Figure 30: Simulated source for noise analysis, standard polarity.

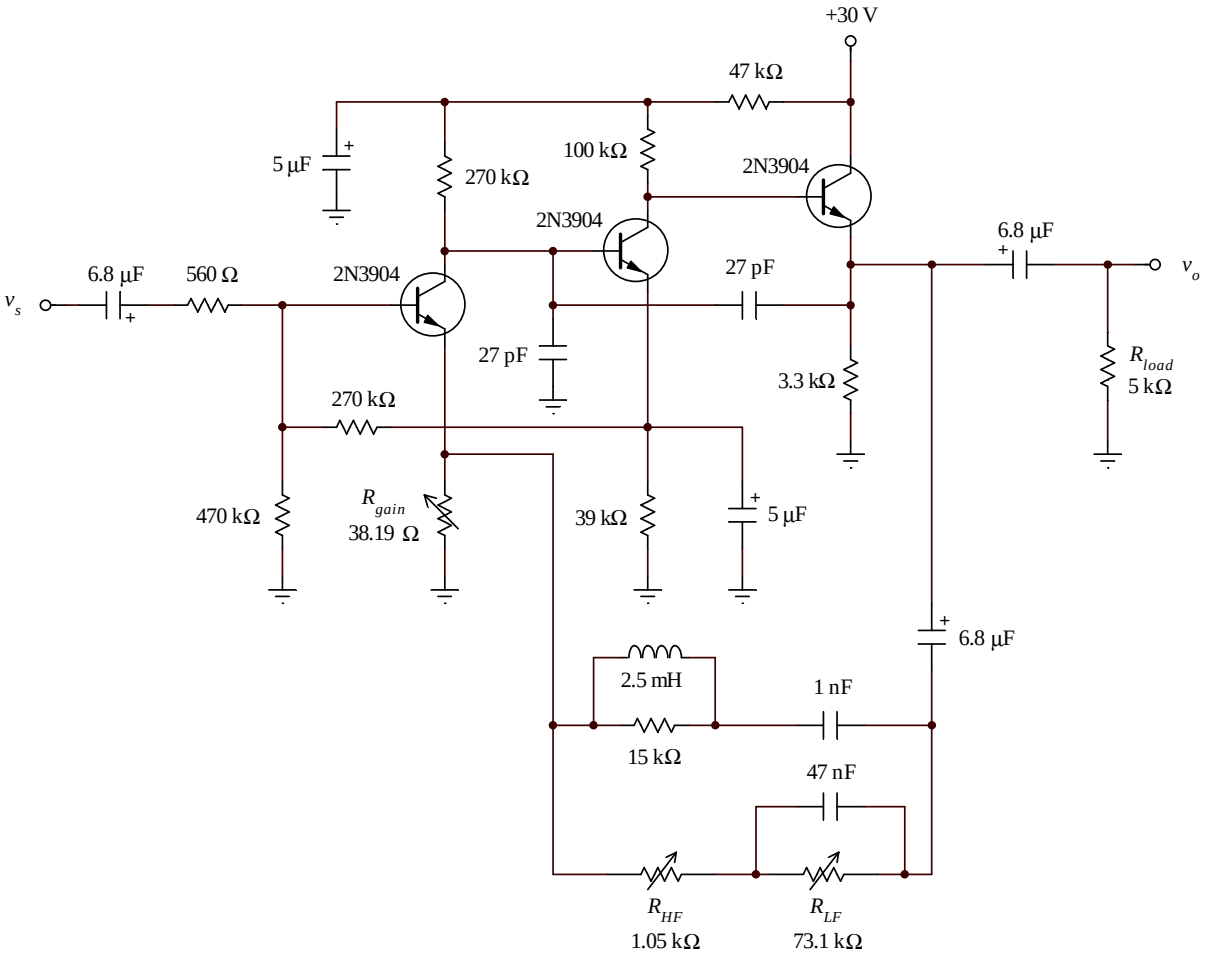

Figure 31: Simulated Crown SXA playback preamplifier circuit.

5.1.1 Crown International SXA Series Playback Preamplifier

The playback section of a Crown SXA 1/4-inch tape recorder is chosen for SPICE simulation. Although no longer in production, this design represents the final generation of mass-produced analog discrete-transistor playback circuits. Due to its prevalence in the resale market, this type of circuit will simulated to provide a baseline for performance. The SPICE model of the Crown SXA playback preamplifier is shown in Fig. 31. This design incorporates both voltage integration and NAB equalization within the feedback loop, as described in Section 2.1.

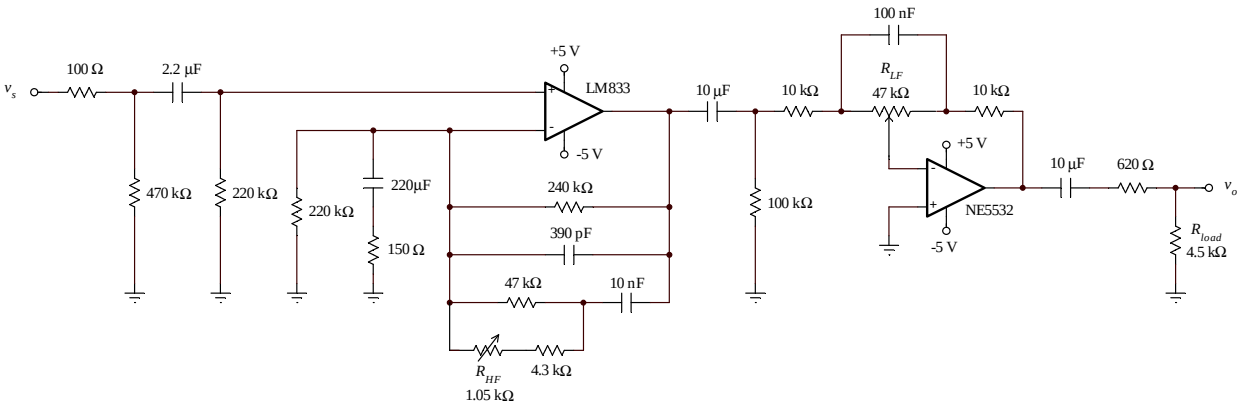

Figure 32: Simulated Otari MX-5050 playback preamplifier circuit.

5.1.2 Otari MX-5050

The Otari MX-5050 is an industry-standard 1/4-inch analog recorder/reproducer currently in production. It utilizes an op-amp-based preamplifier circuit for playback, with voltage integration and NAB equalization executed via the feedback network of the initial non-inverting gain stage. An additional inverting stage provides low-frequency compensation to adjust the 50 Hz pole if necessary. The simulated SPICE circuit is shown in Fig. 32. The Otari MX-5050 represents the current state-of-the-art for 1/4-inch analog machines, and is therefore an important benchmark for comparison.

5.1.3 Original Transresistance Preamplifier Design

The transresistance playback preamplifier design originally suggested by Tritschler is shown in Fig. 33. The expanded design proposed by the research features a few notable modifications. Therefore, for the purposes of validation, the original design is also simulated and analyzed as per Section 4.2.

As can be seen in the SPICE circuit, the original design variation utilizes LM741 op-amps which are generally not suitable for high-fidelity audio applications. Additionally, this circuit accommodates a non-inverting input and thus uses an inverting second stage with shunt-shunt feedback to provide the necessary boost at 3.183 kHz.

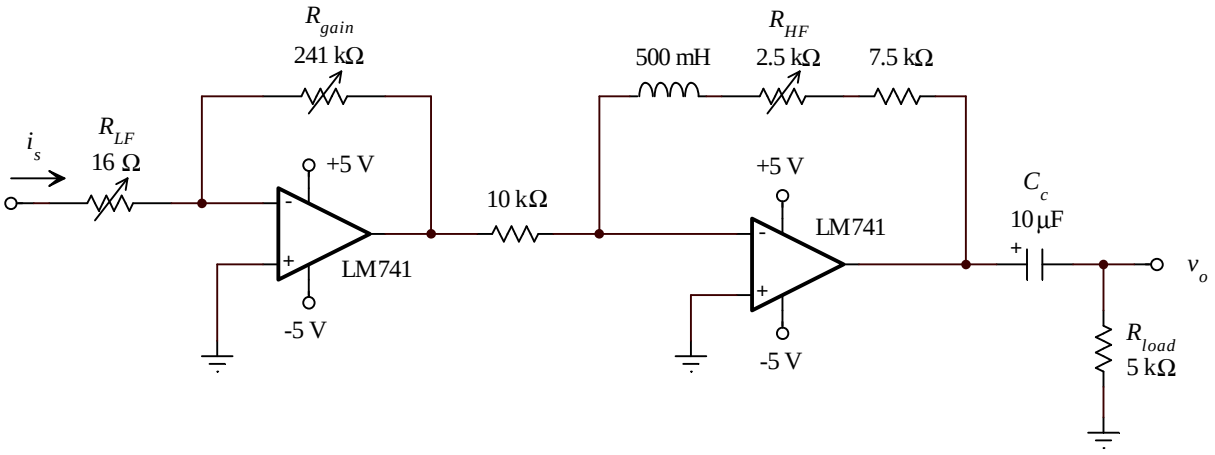

Figure 33: Original transresistance playback preamplifier design as simulated in SPICE.

Shunt-shunt feedback requires a series RL network to accomplish this equalization, rather than an RC network. This, in turn, drives the amplifier towards open-loop until the gain bandwidth product is reached and can result in a significant resonant peak in the output response. Furthermore, the inclusion of a 500-mH inductor greatly increases production costs and consumes valuable surface area on the circuit board. For these reasons, the proposed design utilizes more suitable op-amps and a non-inverting series-shunt boost stage with RC instead of RL filtering.

5.2 Frequency Response

Fig. 34 shows the magnitude response of all three simulated existing designs. Midband gain of all designs is 106.84 dB with respect to the input current. The Crown circuit's response is preferable as it is maintained flat within ±0.43 dB, while the transfer characteristics of the other circuits vary ±1 dB or more.

Fig. 35 depicts the simulated phase response. The angle of the commercially-available circuits varies by nearly ±40°, while the original transresistance preamplifier exhibits a maximum shift of +23°, identical to that of the proposed redesign. Note

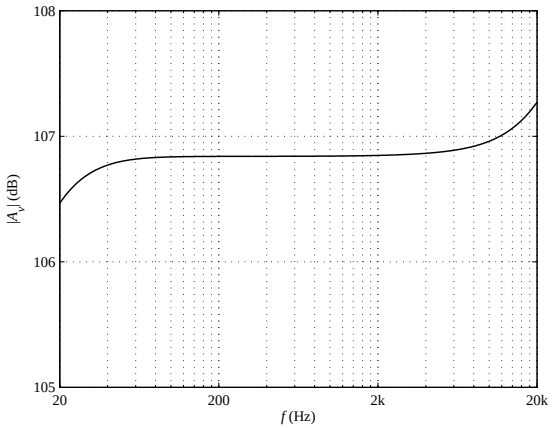

(a)

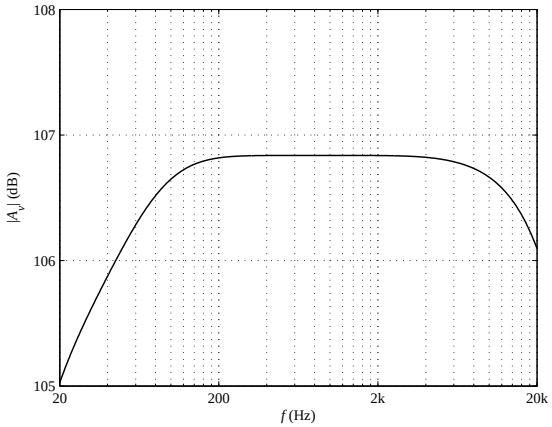

(b)

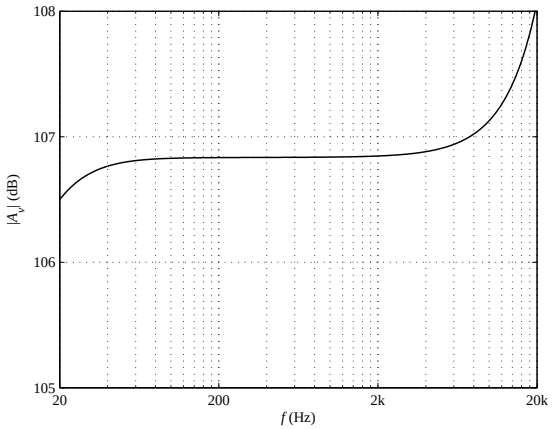

(c)

Figure 34: Simulated magnitude response of existing designs. (a) Crown SXA. (b) Otari MX-5050. (c) Original transresitance preamplifier.

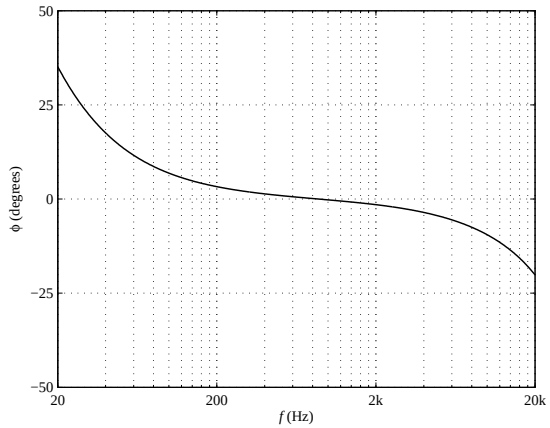

(a)

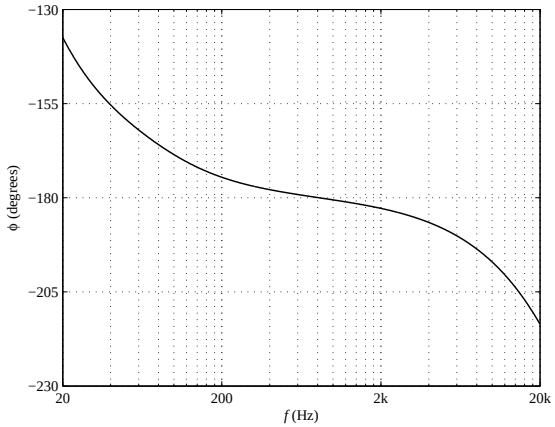

(b)

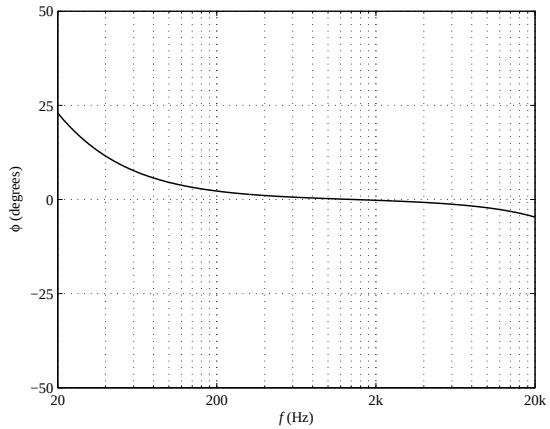

(c)

Figure 35: Simulated phase response of existing designs. (a) Crown SXA. (b) Otari MX-5050. (c) Original transresistance preamplifier.

that the Otari circuit exhibits a net phase of $-180°$ due to the inversion of its second stage.

5.3 Transient Analysis

The 1-kHz sine and 20-kHz square wave transient responses of all three baseline designs are shown in Fig. 36 and Fig. 37, respectively. Although slightly overdamped, the Otari playback preamplifier arguably provides the best step response of the three baseline designs; steady-state peak output is 210.64 mV, or 148.94 mV(rms), with a rise time of 7.95 μs and phase shift of $-208.7°$. Also of note is the severely distorted response of the original transresistance preamplifier at 20 kHz.

5.4 THD and Spectral Analysis

The harmonic spectrum of each amplifier with a sine wave input of 1 kHz is obtained via Fourier analysis. The results are shown in Fig. 38. The spectrum of the Crown circuit and the original transresistance preamplifier are dominated by the 2^{nd} harmonic, whereas the Otari exhibits a more gradual harmonic decay. For this reason, the Otari also has the least overall distortion at 1 kHz.

Fig. 39 compares the spectral response of THD across the audio band. This data indicates that the Crown SXA circuit introduces distortion that increases at both lower and higher frequencies. The Otari exhibits a similar trend, albeit to a lesser extent as the low end approaches 20 Hz. The THD spectrum of the original transresistance preamplifier is largely flat; however, an exponential increase in distortion is observed above 5 kHz. All existing designs therefore exhibit some degree of spectral discontinuity.

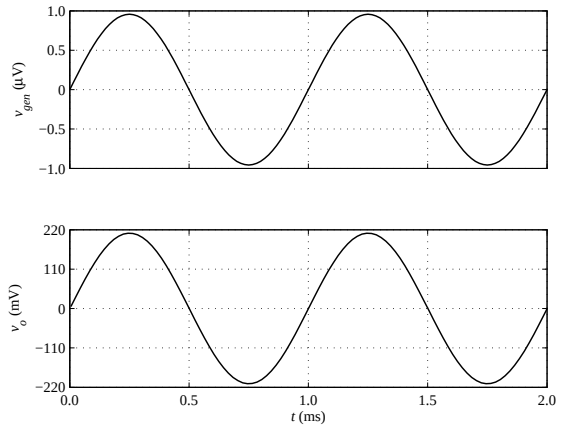

(a)

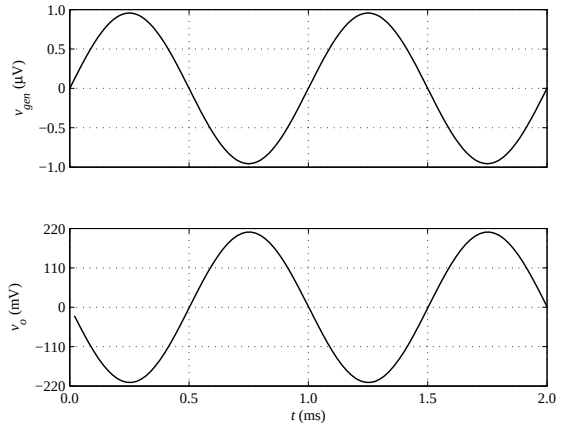

(b)

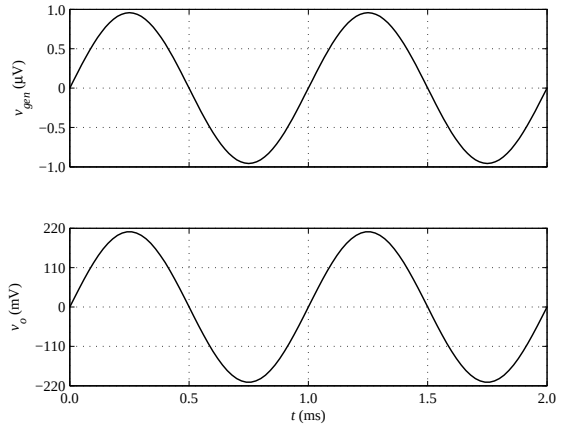

(c)

Figure 36: Simulated transient response of existing designs, 1-kHz sine wave input. (a) Crown SXA. (b) Otari MX-5050. (c) Original transresistance preamplifier.

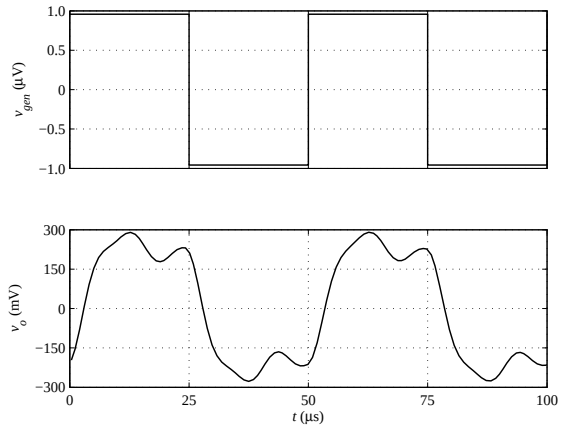

(a)

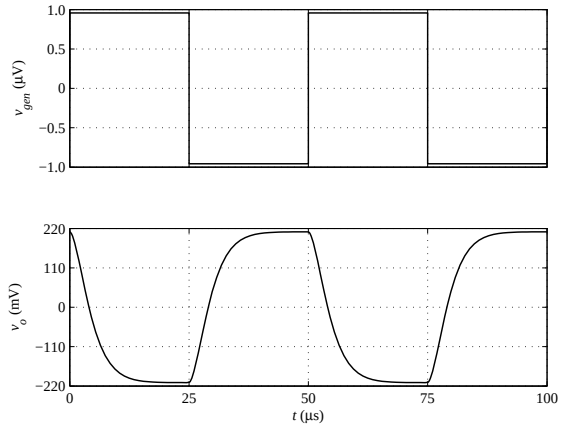

(b)

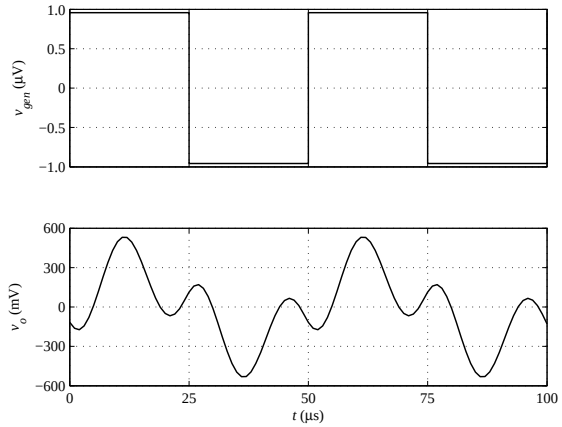

(c)

Figure 37: Simulated transient response of existing designs, 20-kHz square wave input. (a) Crown SXA. (b) Otari MX-5050. (c) Original transresistance preamplifier.

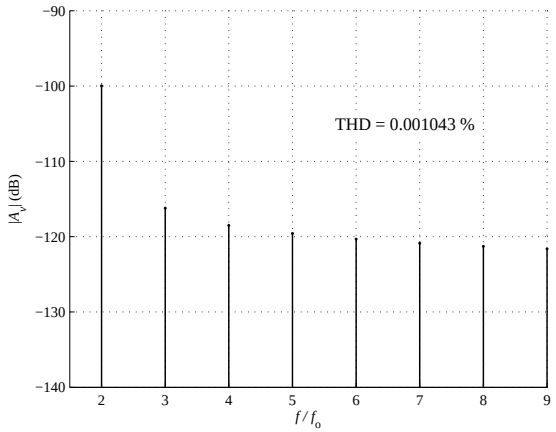

(a)

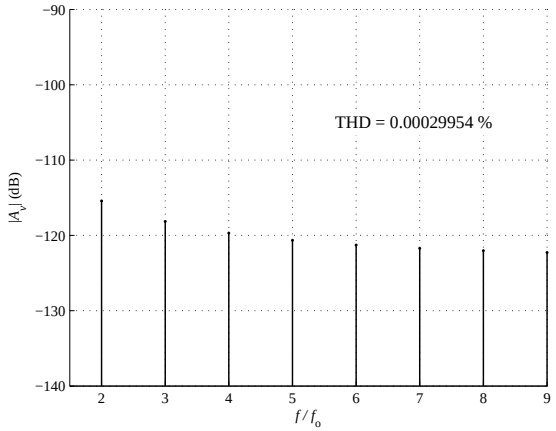

(b)

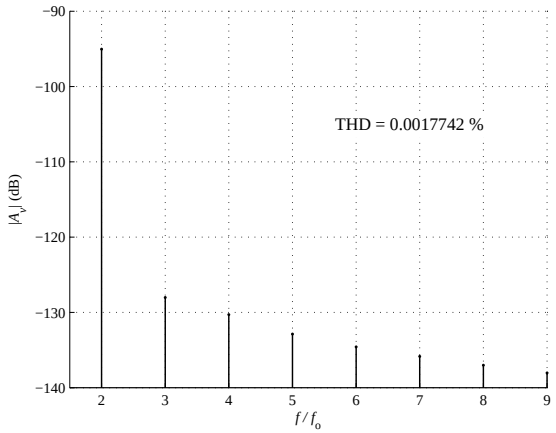

(c)

Figure 38: Harmonic spectrum and THD of simulated existing designs at $f_o = 1$ kHz. (a) Crown SXA. (b) Otari MX-5050. (c) Original transresistance preamplifier.

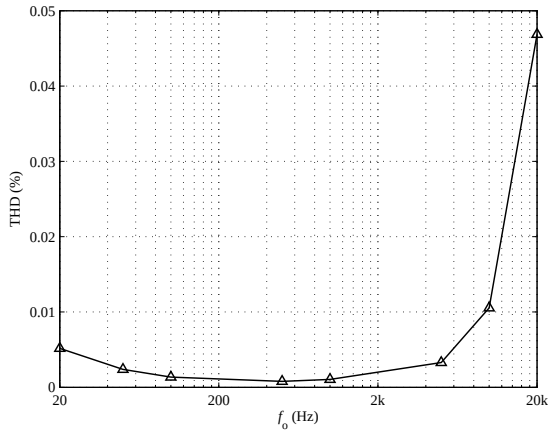

(a)

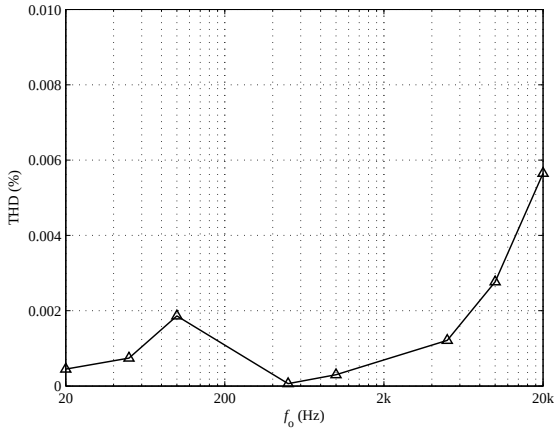

(b)

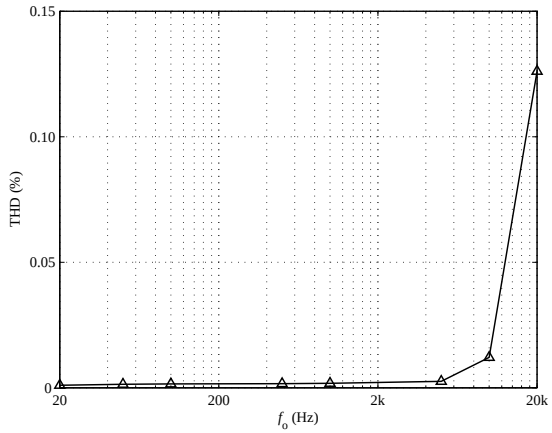

(c)

Figure 39: Effect of fundamental frequency f_o on THD of simulated existing designs. (a) Crown SXA. (b) Otari MX-5050. (c) Original transresistance preamplifier.

5.5 Noise Analysis

The SNR spectrum of each of the three existing designs is obtained in SPICE and the data is presented in Fig. 40. The shape of each characteristic is nearly identical to that of the proposed design, indicating that all simulated designs introduce noise in direct proportion to frequency. However, this characteristic is shifted vertically in each case, varying the midband SNR. The Crown SXA circuit exhibits the best noise suppression with a SNR of nearly 72 dB at 1 kHz. The Otari preamplifier contributes the most noise with a midband SNR of 66.5 dB. The original transresistance preamplifier is comparable to the proposed re-design, with a SNR of 67.5 dB at midband.

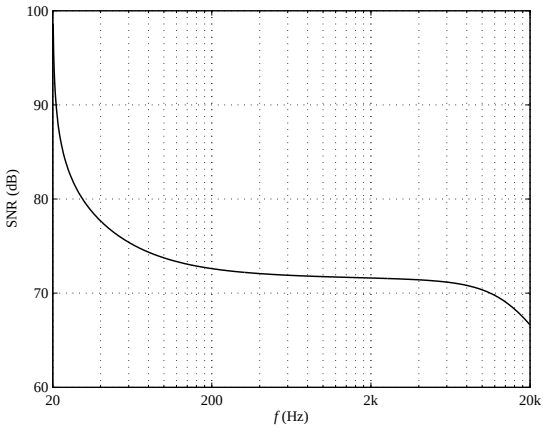

(a)

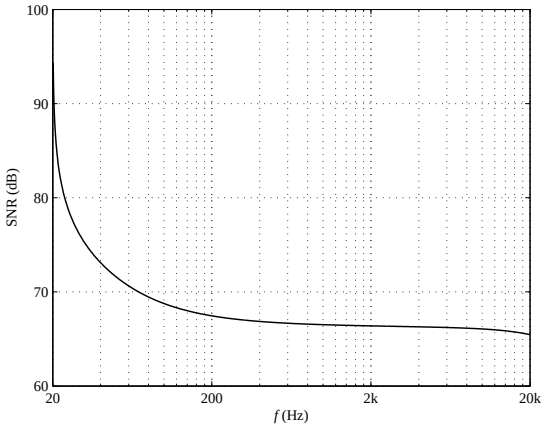

(b)

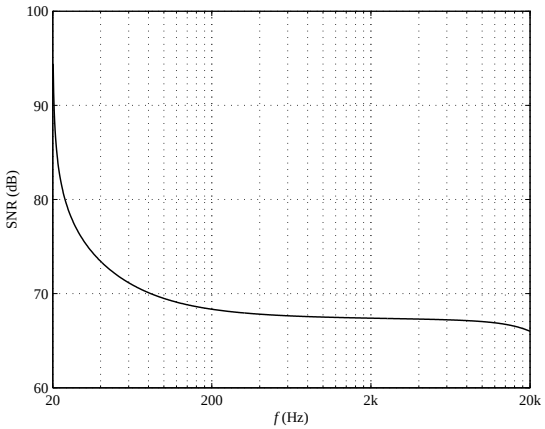

(c)

Figure 40: Noise analysis of simulated existing designs. (a) Crown SXA. (b) Otari MX-5050. (c) Original transresistance preamplifier.

6 Conclusions and Future Work

6.1 Performance Comparison

A side-by-side comparison of nearly all simulation results indicates that superior performance is possible via the proposed transresistance preamplifier design. The magnitude response of the proposed circuit seen in Fig. 24(a) is noticeably flatter than that of existing designs and is also more stable within 0.34 dB. Even if the spectrum is expanded beyond the nominal audio band, as shown in Fig. 41, the proposed design outperforms all other variations.

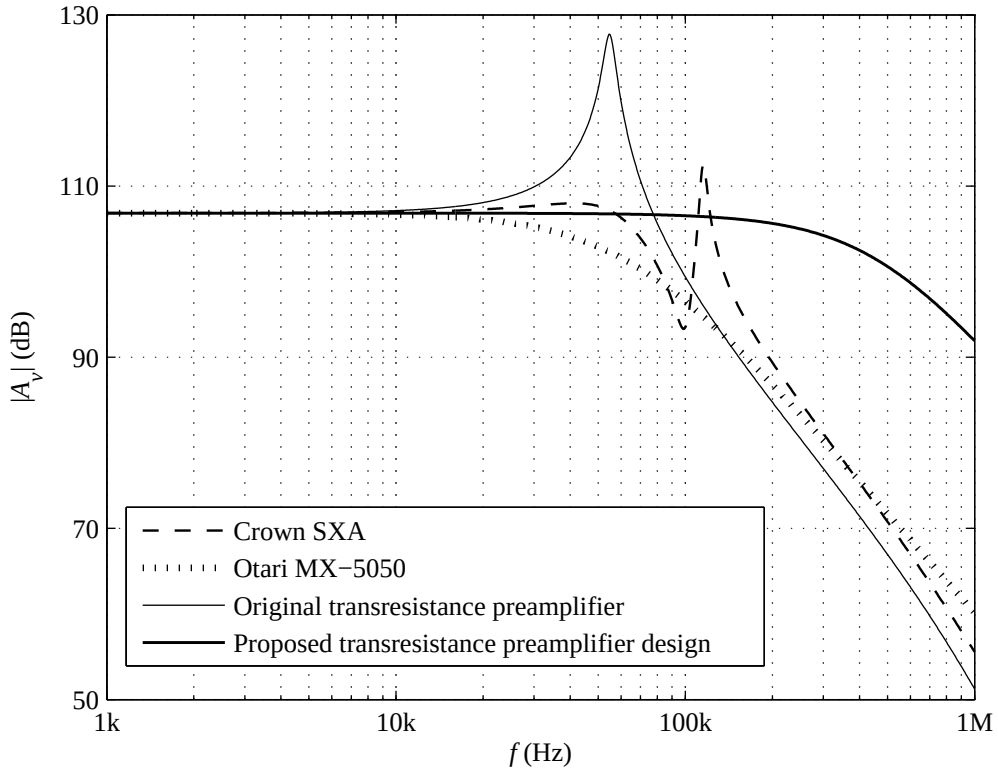

Figure 41: Comparison of extended magnitude response.

This is important in that audible fidelity is subject to the effects of harmonic frequencies beyond human hearing, as demonstrated by the work of Hiraga, et al. [14]. Beyond 20 kHz, the proposed design eliminates the harmful resonant peaks of the Crown circuit and Tritschler's initial design. Overall bandwidth has been increased to approximately 320 kHz, an improvement over existing designs which accounts for the superior step response of Fig. 25. In addition, the transresistance topology exhibits a narrower phase margin than existing commercial designs, as can be seen in Fig. 24(b) and Fig. 35.

The proposed design also provides improved performance in terms of harmonic distortion. Amplifiers with low audible distortion will produce a Fourier series with gradually decreasing coefficients [14]. The envelope of the harmonic series in Fig. 26 is evidence that the proposed circuit possesses this characteristic. Not only is the net THD of this design very low, but the frequency-dependent behavior of its distortion is also an improvement over existing designs. Hiraga's study of harmonic frequencies and audible distortion indicates that ideal high-fidelity signal reproduction possesses a *non-dynamic* distortion characteristic; ideally, THD should remain constant regardless of the fundamental frequency [14]. The THD spectrum of the proposed circuit is nearly flat compared to all other simulated designs, as seen in Fig. 42. The analysis also demonstrates that THD of both voltage-integrating amplifiers increases at low frequencies, while THD of both transresistance amplifiers decreases. This justifies the reasoning behind the proposed topology, as it supports the hypothesis that low-frequency boosting increases spectral discontinuity.

The SNR of the proposed design is 67.6 dB at midband. This is nominally better than the original transresistance preamplifier and a marginal improvement over the Otari MX-5050, but measurably less than the Crown SXA with a midband SNR of 71.8 dB. However, simulated noise performance is comparable among the three op-amp-based designs. This may indicate that topology itself has relatively little effect

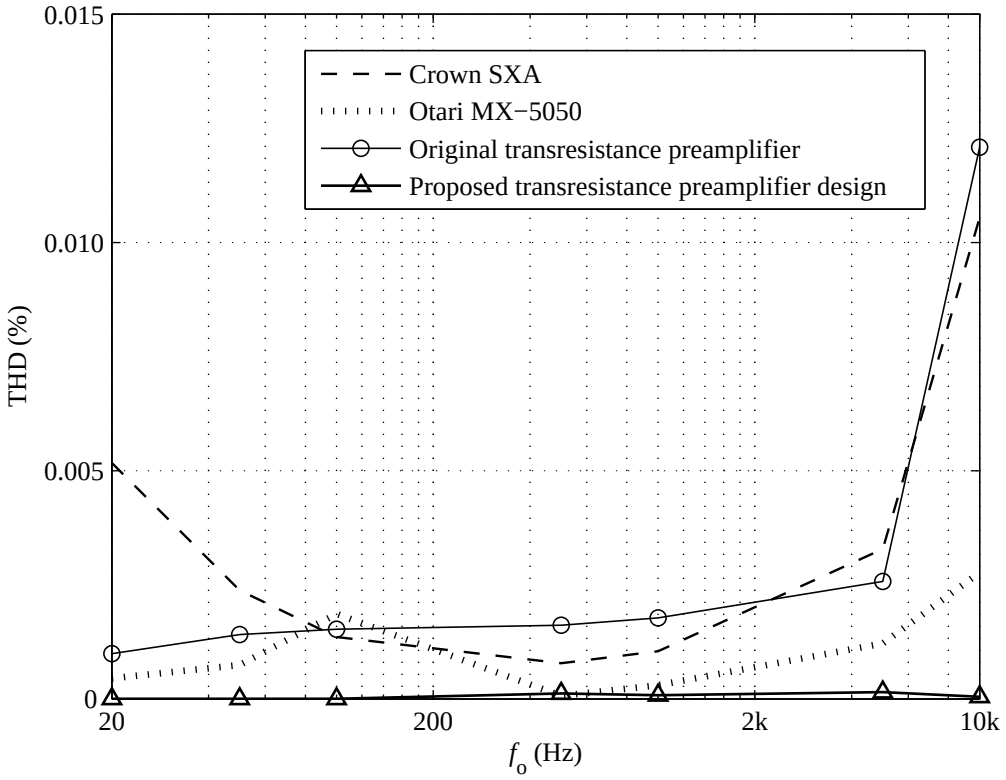

Figure 42: Comparison of THD spectra.

on SNR; rather, in this application, noise may chiefly be a function of the active device(s). It should likewise be pointed out that noise performance of the medium as a whole is generally limited by the tape substrate. Analog magnetic tape currently in production has a maximum SNR of 66 dB at operating speeds of at 15 ips, due to record bias noise [18], [19]. As long as the SNR of the playback preamplifier is greater, the electronics do not contribute audible noise.

The design enhancements of the proposed circuit, vis-á-vis Tritschler's original preamplifier, are justified by the simulation results. Step response, magnitude response, and THD are significantly improved, with no appreciable difference in the phase margin. When further viewed in the context of eliminating the need for a discrete inductor in the second stage, the proposed redesign presents a clear improvement over the original circuit.

Although not directly performance-related, an additional benefit of the proposed transresistance preamplifier is a significant reduction in circuit size and complexity versus traditional voltage-integrating topologies. The proposed design utilizes nearly 75% fewer passive components than the two commercially-available designs examined, requiring no discrete inductors and only one electrolytic capacitor.

6.2 Summary of Results

Table I presents an overview of the numerical results obtained from SPICE simulation. Table II shows the error between calculated design parameters and simulation results. With the exception of f_{H2}, all discrepancies derive from adjustable settings, and are small enough to validate the design procedure as presented. It should be noted that f_{H2} still falls within 0.5% of the acceptable specified value; however, for better accuracy, an improved design equation may be required as described in Section 6.3.4.

Table 1

Summary of Simulation Results

			Transresistance preamplifier	
	Crown SXA	Otari MX-5050	Original	Proposed
Maximum magnitude deviation	+0.43 dB	-1.81 dB	+1.23 dB	-0.34 dB
Maximum phase margin	+35.16°	+42.46°(−180°)	+22.98°	+22.97°
Phase, 1 kHz	-0.23°	-0.56°(−180°)	+0.23°	+0.22°
Phase, 20 kHz	-24.93°	-28.70°(−180°)	-4.69°	-4.77
THD, 1 kHz	0.00143 %	0.00030 %	0.00177 %	0.00008 %
SNR, 1 kHz	+71.8 dB	+66.5 dB	+67.5 dB	+67.6 dB

Table 2

Validation of Design Procedure

	Theoretical	Simulated	Error	Notes
$f_{NAB,low}$	50.00 Hz	51.11 Hz	+2.22 %	$R_{50\text{Hz}} = 5.664\,\Omega$
$f_{NAB,high}$	3182.59 Hz	3178.89 Hz	-0.12 %	$R_2 = 10.5\,\text{k}\Omega$
f_{H2}	241.877 kHz	199.136 kHz[1]	-17.67 %	≥200 kHz specified
$\frac{v_o}{i_s}$	106.848 dB	106.836 dB	-0.01 %	f = 1 kHz
$v_{o(rms)}$	148.810 mV	148.404 mV	-0.27 %	$v_{s(rms)}$= 1.7 mV

SPICE simulation has shown that the proposed transresistance playback preamplifier design provides the following performance benefits over existing designs:

- Improved step response.
- Improved magnitude and phase response.
- Reduced THD.
- Improved harmonic distortion spectrum.
- Significant reduction in circuit size and complexity.

[1]Measured via extended AC analysis of circuit in Fig. 23

6.3 Future Work

6.3.1 Practical Implementation

Simulation of the proposed design has proven promising enough to warrant fabrication and testing of a prototype circuit. This introduces the only potential difficulty in realizing the proposed approach, namely that a correctly-matched reproduce head is required for the preamplifier circuit to yield the benefits described in the previous sections. Although a wide range of reproduce heads are commercially available, the present research has been unable to locate one with the correct combination of inductance and series resistance currently in production. A custom reproduce head will therefore need to be fabricated to the desired specifications of $L_s = 400$ mH and $r_{DC} = 120\,\Omega$. Correspondence with JRF Magnetic Sciences, a manufacturer of custom-specification tape heads, has indicated that this is feasible with current technology.

In the event that a prototype reproduce head is prohibitively expensive or unavailable, the proposed design should be simulated in SPICE using a model of the Nortronics WP-B1HY7K, a commercially-available reproduce head with $L_s = 400$ mH and $r_{DC} = 140\,\Omega$. Despite a degradation of low-frequency response due to the larger series resistance, an improvement in THD consistent with that of the 120-Ω head may nonetheless warrant construction of a prototype using the stock part.

6.3.2 Higher Gain Configuration

An additional promising feature of the proposed transresistance amplifier is stable simulated performance at high gain. Increasing the transresistance of the first stage by a factor of ten provides a line-level output voltage sufficient for driving a power amplifier or headphones. Initial simulations indicate a 1.5-V(rms) output may be obtained with no major impact on other performance parameters, provided supply volt-

ages are also increased. Low-frequency response suffers slightly, but can be restored by further reducing the series resistance of the reproduce head. Further simulation and analysis is suggested to confirm whether the proposed design may be modified in this manner to function as both preamplifier and line amplifier.

6.3.3 Bandwidth Reduction

Although the nominal limit of human hearing is 20 kHz, Hiraga's work presents a strong argument for the preservation of harmonics beyond this frequency [14]. The proposed design therefore features a total bandwidth of approximately 325 kHz, as seen in Fig. 41. However, this number may be excessive in practice and warrants further examination, particularly given the overshoot of the step response in Fig. 25(b). The damping can theoretically be improved by reducing bandwidth. Construction of a prototype circuit may also necessitate bandwidth reduction if the preamplifier exhibits instability due to high current-to-voltage gain. Effective bandwidth can be decreased via R_1 per (4.14), provided similar adjustment is made to R_2 to preserve the NAB boost frequency. Initial simulation indicates that reducing total bandwidth to 100 kHz yields a critically-damped step response with no significant increase in THD. In light of this fact, (4.17) may need to be revised to constrain the design to minimal optimum bandwidth.

6.3.4 Design Calculation for Second Stage Stop-Boost Frequency

Table II shows all design calculations to be accurate except for (4.18). This is most likely because the bandwidth of each op-amp has been neglected; both are assumed to be large enough so as not to interact with the upper shelving frequency f_{H2}. However, simulation indicates that this may not be the case since high-frequency boosting ceases below the theoretical value of f_{H2}.[2] Although the "stop-boost" frequency does not

[2] As determined via extended AC analysis of circuit shown in Fig. 23.

necessarily equal the total bandwidth, as demonstrated by Fig. 41, a more accurate design equation is needed in lieu of (4.18). This expression must take into account not only f_{H2}, but also the effective bandwidth of each op-amp. The latter is not easily derived in the case of the second stage. Since the gain of the active high-pass shelving filter is dynamic, bandwidth cannot be calculated simply as the ratio of unity-gain bandwidth to A_{v2}.

References

[1] F. Rumsey and T. McCormick, *Sound and Recording*, 6th ed. Oxford: Focal Press, 2009, p. 168.

[2] E. D. Daniel, C. D. Mee, and M. H. Clark, Eds., *Magnetic Recording: The first 100 years*. Piscataway, NJ: IEEE Press, 1999, p. 108.

[3] D. M. Huber and R. E. Runstein, *Modern Recording Techniques*, 6th ed. Burlington, MA: Focal Press, 2005, pp. 187-209.

[4] C. P. Boegli. "The anode follower," *Audio*, vol. 44, no. 12, pp. 19-22, Dec. 1960.

[5] A. J. Perandi, "Vacuum tube and MOSFET transimpedance amplifier," U.S. Patent 5,017,884, May 21, 1991.

[6] J. Tritschler, "An improved playback amplifier for high-fidelity analog recording systems," Wright State University, Dayton, OH, USA, technical report, 2000.

[7] Catalog No. 7079 R-049, *Nortronics Magnetic Head Specifications*, Nortronics Co. Inc., Minneapolis, MN.

[8] G. Ballou, Ed., *Handbook for Sound Engineers*, 2nd ed. Newton, MA: Focal Press, 1998.

[9] Crown International Technical Staff, *SXA Series*, Crown International, 1975.

[10] Otari Inc. Technical Staff, *MX-5050BII Series Professional Recorders*, Otari Inc., 1983.

[11] TEAC Corporation Technical Staff, *TASCAM 32 2-Track Recorder / Reproducer*, TEAC Corporation, 1986.

[12] S. J. Tritschler, "The concept, design, and construction of a sigma-transadmittance amplifier for audio-frequency analog magnetic tape recording," M.S. thesis, Wright State University, Dayton, OH, USA, 2003.

[13] J. M. Woram, *Sound Recording Handbook*. Indianapolis: Howard W. Sams & Company, 1989, pp. 331-378.

[14] J. Hiraga. "Harmony and distortion, part 2," *audioXpress*, vol. 2, no.3, pp. 48-53, Mar. 2002.

[15] M. Jones, *Valve Amplifiers*, 2nd ed. Oxford: Newnes, 1999, pp. 122-147.

[16] Texas Instruments, "Stability analysis of voltage-feedback op-amps," Appl. Report SLOA020-A, pp. 7-14.

[17] C. W. Lander, *Power Electronics*, 2nd ed. Berkshire, England: McGraw-Hill (UK), 1987, p. 261.

[18] RGM International, "Technical data: Studio Master 900," SM 900 datasheet, April 2006.

[19] ATR Magnetics, "ATR master tape specifications," *ATR Magnetics, LLC.* [Online]. Available: http://www.atrtape.com. [Accessed: Jul. 28, 2010].

Appendix A

SPICE code used for simulation of the proposed transresistance preamplifier, with equalized current source to model tape signal for AC, transient, and Fourier analyses.

```
****************************************
** This file was created by TINA **
** (c) 1996-2006 DesignSoft, Inc.  **
****************************************
.LIB "F:\Program Files\DesignSoft\Tina 7\EXAMPLES\SPICE\TSPICE.LIB"
.LIB "F:\Program Files\DesignSoft\Tina 7\SPICELIB\TI.LIB"
.LIB "F:\Program Files\DesignSoft\Tina 7\SPICELIB\Operational Amplifiers.LIB"
.LIB
.TEMP 27
.AC DEC 333 20 20K
.TRAN 204U 102M 100M
.DC LIN Vgen 0 1 10M
.OPTIONS ABSTOL=1U ITL1=100 ITL2=40 ITL4=20
.PROBE V(13,0)
Vgen 16 0 DC 0 AC 1 0
+ SIN( 0 957N 1K 0 0 0 )
VNegVcc 4 0 -5
VPosVcc 3 0 5
XU1 0 1 3 4 2 6 5 NE5534_0
XU2 2 7 3 4 8 10 9 NE5534_0
R50Hz 11 1 3
C1 7 12 4.7N IC=0
Cc 8 13 10U IC=0
***** Current source for reverse-polarity reproduce head *****
GVCCS1 15 0 14 0 1
Ra 16 17 1K
EVCVS1 18 0 17 0 10
Ca 17 0 50N IC=0
Rb1 18 14 9K
Rb2 19 0 1K
Cb 14 19 3.183U IC=0
************************************************************
Rf 1 2 220K
R1 12 0 140
Rload 13 0 5K
R2 7 8 10.5K
```

```
Rdc 11 15 120
Ls 15 0 400M IC=0
***** NE5534 SOURCE: TEXAS INSTRUMENTS *****
* C2 ADDED TO SIMULATE UNCOMPENSATED FREQUENCY RESPONSE (UWE BEIS)
* NE5534 OPERATIONAL AMPLIFIER "MACROMODEL" SUBCIRCUIT
* CREATED USING PARTS RELEASE 4.01 ON 04/10/89 AT 12:41
* (REV N/A) SUPPLY VOLTAGE: +/-15V
* CONNECTIONS:
* 1 = NON-INVERTING INPUT
* 2 = INVERTING INPUT
* 3 = POSITIVE POWER SUPPLY
* 4 = NEGATIVE POWER SUPPLY
* 5 = OUTPUT
* 6,7 = COMPENSATION
*****************************************
.SUBCKT NE5534_0 1 2 3 4 5 6 7
C1 11 12 7.703E-12
C2 6 7 3.500E-12
DC 5 53 DX
DE 54 5 DX
DLP 90 91 DX
DLN 92 90 DX
DP 4 3 DX
EGND 99 0 POLY(2) (3,0) (4,0) 0 .5 .5
FB 7 99 POLY(5) VB VC VE VLP VLN 0 2.893E6 -3E6 3E6 3E6 -3E6
GA 6 0 11 12 1.382E-3
GCM 0 6 10 99 13.82E-9
IEE 10 4 DC 133.0E-6
HLIM 90 0 VLIM 1K
Q1 11 2 13 QX
Q2 12 1 14 QX
R2 6 9 100.0E3
RC1 3 11 723.3
RC2 3 12 723.3
RE1 13 10 329
RE2 14 10 329
REE 10 99 1.504E6
RO1 8 5 50
RO2 7 99 25
RP 3 4 7.757E3
VB 9 0 DC 0
VC 3 53 DC 2.700
VE 54 4 DC 2.700
VLIM 7 8 DC 0
VLP 91 0 DC 38
VLN 0 92 DC 38
.MODEL DX D(IS=800.0E-18)
```

```
.MODEL QX NPN(IS=800.0E-18 BF=132)
.ENDS
.END
```

Appendix B

SPICE code used for simulation of the proposed transresistance preamplifier, with unequalized current source for standalone noise analysis and extended AC analysis of playback characteristic.

```
*****************************************
** This file was created by TINA **
** (c) 1996-2006 DesignSoft, Inc.  **
*****************************************
.LIB "F:\Program Files\DesignSoft\Tina 7\EXAMPLES\SPICE\TSPICE.LIB"
.LIB "F:\Program Files\DesignSoft\Tina 7\SPICELIB\TI.LIB"
.LIB "F:\Program Files\DesignSoft\Tina 7\SPICELIB\Operational Amplifiers.LIB"
.LIB
.TEMP 27
.AC DEC 166 10 10MEG
.TRAN 510U 255M 250M
.DC LIN Is 0 1 10M
.OPTIONS ABSTOL=1U ITL1=100 ITL2=40 ITL4=20
.PROBE V(4,0)
Is 3 0 DC 0 AC 1 0
+ SIN( 0 957N 400 0 0 0 )
VNegVcc 9 0 -5
VPosVcc 8 0 5
R50Hz 1 2 3
Ls 3 0 400M IC=0
Rdc 1 3 120
Rload 4 0 5K
Cc 5 4 10U IC=0
XU2 6 7 8 9 5 11 10 NE5534_0
Rf 2 6 220K
XU1 0 2 8 9 6 13 12 NE5534_0
R1 14 0 140
C1 7 14 4.7N IC=0
R2 7 5 10.5K
***** NE5534 SOURCE: TEXAS INSTRUMENTS *****
* C2 ADDED TO SIMULATE UNCOMPENSATED FREQUENCY RESPONSE (UWE BEIS)
* NE5534 OPERATIONAL AMPLIFIER "MACROMODEL" SUBCIRCUIT
* CREATED USING PARTS RELEASE 4.01 ON 04/10/89 AT 12:41
* (REV N/A) SUPPLY VOLTAGE: +/-15V
```

```
* CONNECTIONS:
* 1 = NON-INVERTING INPUT
* 2 = INVERTING INPUT
* 3 = POSITIVE POWER SUPPLY
* 4 = NEGATIVE POWER SUPPLY
* 5 = OUTPUT
* 6,7 = COMPENSATION
*****************************************
.SUBCKT NE5534_0 1 2 3 4 5 6 7
C1 11 12 7.703E-12
C2 6 7 3.500E-12
DC 5 53 DX
DE 54 5 DX
DLP 90 91 DX
DLN 92 90 DX
DP 4 3 DX
EGND 99 0 POLY(2) (3,0) (4,0) 0 .5 .5
FB 7 99 POLY(5) VB VC VE VLP VLN 0 2.893E6 -3E6 3E6 3E6 -3E6
GA 6 0 11 12 1.382E-3
GCM 0 6 10 99 13.82E-9
IEE 10 4 DC 133.0E-6
HLIM 90 0 VLIM 1K
Q1 11 2 13 QX
Q2 12 1 14 QX
R2 6 9 100.0E3
RC1 3 11 723.3
RC2 3 12 723.3
RE1 13 10 329
RE2 14 10 329
REE 10 99 1.504E6
RO1 8 5 50
RO2 7 99 25
RP 3 4 7.757E3
VB 9 0 DC 0
VC 3 53 DC 2.700
VE 54 4 DC 2.700
VLIM 7 8 DC 0
VLP 91 0 DC 38
VLN 0 92 DC 38
.MODEL DX D(IS=800.0E-18)
.MODEL QX NPN(IS=800.0E-18 BF=132)
.ENDS
.END
```